

# Uncovering the Limits of Adversarial Training against Norm-Bounded Adversarial Examples

Sven Gowal<sup>1</sup>, Chongli Qin<sup>1</sup>, Jonathan Uesato<sup>1</sup>, Timothy Mann<sup>1</sup> and Pushmeet Kohli<sup>1</sup>

<sup>1</sup>DeepMind

Adversarial training and its variants have become de facto standards for learning robust deep neural networks. In this paper, we explore the landscape around adversarial training in a bid to uncover its limits. We systematically study the effect of different training losses, model sizes, activation functions, the addition of unlabeled data (through pseudo-labeling) and other factors on adversarial robustness. We discover that it is possible to train robust models that go well beyond state-of-the-art results by combining larger models, Swish/SiLU activations and model weight averaging. We demonstrate large improvements on CIFAR-10 and CIFAR-100 against  $\ell_\infty$  and  $\ell_2$  norm-bounded perturbations of size 8/255 and 128/255, respectively. In the setting with additional unlabeled data, we obtain an accuracy under attack of 65.88% against  $\ell_\infty$  perturbations of size 8/255 on CIFAR-10 (+6.35% with respect to prior art). Without additional data, we obtain an accuracy under attack of 57.20% (+3.46%). To test the generality of our findings and without any additional modifications, we obtain an accuracy under attack of 80.53% (+7.62%) against  $\ell_2$  perturbations of size 128/255 on CIFAR-10, and of 36.88% (+8.46%) against  $\ell_\infty$  perturbations of size 8/255 on CIFAR-100. All models are available at [https://github.com/deepmind/deepmind-research/tree/master/adversarial\\_robustness](https://github.com/deepmind/deepmind-research/tree/master/adversarial_robustness).

## 1. Introduction

Neural networks are being deployed in a wide variety of applications with great success (Goodfellow et al., 2016; Hinton et al., 2012; Krizhevsky et al., 2012). As neural networks tackle challenges ranging from ranking content on the web (Covington et al., 2016) to autonomous driving (Bojarski et al., 2016) via medical diagnostics (De Fauw et al., 2018), it has become increasingly important to ensure that deployed models are robust and generalize to various input perturbations. Despite their success, neural networks are not intrinsically robust. In particular, the addition of small but carefully chosen deviations to the input, called adversarial perturbations, can cause the neural network to make incorrect predictions with high confidence (Carlini & Wagner, 2017a; Goodfellow et al., 2015; Kurakin et al., 2016; Szegedy et al., 2014). Starting with Szegedy et al. (2014), there has been a lot of work on understanding and generating adversarial perturbations (Athalye & Sutskever, 2018; Carlini & Wagner, 2017b), and on building models that are robust to such perturbations (Goodfellow et al., 2015; Kannan et al., 2018; Madry et al., 2018; Papernot et al., 2016). Robust optimization techniques, like the one developed by Madry et al. (2018), learn robust models by finding worst-case adversarial examples (by running an inner optimization procedure) at

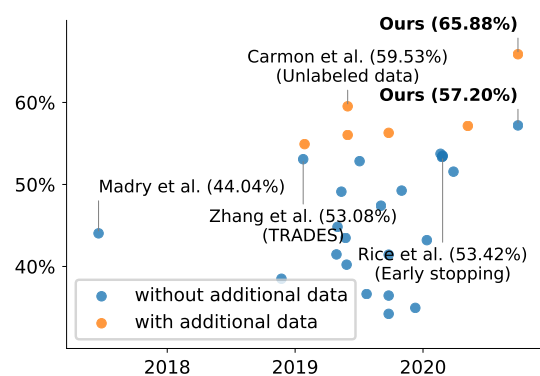


Figure 1 | Accuracy of various models ordered by publication date against AUTOATTACK (Croce & Hein, 2020) on CIFAR-10 with  $\ell_\infty$  perturbations of size 8/255. Our newest models (on the far right) improve robust accuracy by +3.46% without additional data and by +6.35% when using additional unlabeled data.

each training step and adding them to the training data. This technique has proven to be effective and is now widely adopted.

Since Madry et al. (2018), various modifications to their algorithm have been proposed (Andriushchenko & Flammarion, 2020; Huang et al., 2020; Pang et al., 2020b; Qin et al., 2019; Xie et al., 2019; Zoran et al., 2019). We highlight the work by Zhang et al. (2019) who proposed TRADES which balances the trade-off between standard and robust accuracy, and the work by Carmon et al. (2019); Najafi et al. (2019); Uesato et al. (2019); Zhai et al. (2019) who simultaneously proposed the use of additional unlabeled data in this context. As shown in Figure 1, despite this flurry of activity, progress over the past two years has been slow. In a similar spirit to works exploring transfer learning (Raffel et al., 2020) or recurrent architectures (Jozefowicz et al., 2015), we perform a systematic study around the landscape of adversarial training in a bid to discover its limits. Concretely, we study the effects of (i) the objective used in the inner and outer optimization procedures, (ii) the quantity and quality of additional unlabeled data, (iii) the model size, as well as (iv) other factors (such as the use of model weight averaging). In total we trained more than 150 adversarially robust models and dissected each of them to uncover new ideas that could improve adversarial training and our understanding of robustness. Here is a non-exhaustive list highlighting our findings (in no specific order):

- TRADES (Zhang et al., 2019) combined with early stopping outperforms regular adversarial training (as proposed by Madry et al., 2018). This is in contrast to the observations made by Rice et al. (2020) (subsection 4.1).
- As observed by Madry et al. (2018); Uesato et al. (2019); Xie & Yuille (2019), increasing the capacity of models improves robustness (subsection 4.4).
- The choice of activation function matters. Similar to observations made by Xie et al. (2020b), we found that Swish/SiLU (Elfwing et al., 2018; Hendrycks & Gimpel, 2016; Ramachandran et al., 2017) performs best. However, in contrast to Xie et al., we found that other “smooth” activation functions do not necessarily improve robustness (subsubsection 4.5.2).
- The way in which additional unlabeled data is extracted from the 80 Million Tiny Images dataset (80M-TI) (Torralba et al., 2008) and used during training can have a significant impact (subsection 4.3).
- Model weight averaging (WA) (Izmailov et al., 2018) consistently provides a boost in robustness. In the setting without additional unlabeled data, WA provides improvements as large as those provided by TRADES on top of classical adversarial training (subsubsection 4.5.1).

These findings result in a suite of models that significantly improve on the state-of-the-art against  $\ell_\infty$  and  $\ell_2$  norm-bounded perturbations on CIFAR-10, and against  $\ell_\infty$  norm-bounded perturbations on CIFAR-100 and MNIST (as measured by AUTOATTACK):<sup>1</sup>

- On CIFAR-10 against  $\ell_\infty$  norm-bounded perturbations of size  $\epsilon = 8/255$ , we train models with 65.88% and 57.20% robust accuracy with and without additional unlabeled data, respectively (at the time of writing, prior art was 59.53% and 53.74% in both settings).
- With the same settings used for CIFAR-10 against  $\ell_\infty$  norm-bounded perturbations, on CIFAR-10 against  $\ell_2$  norm-bounded perturbations of size  $\epsilon = 128/255$ , we train models with 80.53% and 74.50% robust accuracy with and without additional unlabeled data, respectively (prior art was 72.91% and 69.24%).
- On CIFAR-100 against  $\ell_\infty$  norm-bounded perturbations of size  $\epsilon = 8/255$ , we train models with 36.88% and 30.03% robust accuracy with and without additional unlabeled data, respectively (prior art was 28.42% and 18.95%).

<sup>1</sup><https://github.com/fra31/auto-attack>

In this study, we aim to find the current limits of adversarial robustness. What we found was that an accumulation of small factors can significantly improve upon the state-of-the-art when combined. As fundamentally new techniques might be needed, it is important to understand the limitations of current approaches. We hope that this new set of baselines can further new understanding about adversarial robustness.

## 2. Background

### 2.1. Context

**Adversarial attacks.** Since Szegedy et al. (2014) observed that neural networks which achieve high accuracy on test data are highly vulnerable to adversarial examples, the art of crafting increasingly sophisticated adversarial examples has received a lot of attention. Goodfellow et al. (2015) proposed the Fast Gradient Sign Method (FGSM) which generates adversarial examples with a single normalized gradient step. It was followed by R+FGSM (Tramèr et al., 2017), which adds a randomization step, and the Basic Iterative Method (BIM) (Kurakin et al., 2016), which takes multiple smaller gradient steps. These are often grouped under the term Projected Gradient Descent (PGD) which usually refers to the optimization procedure used to search norm-bounded perturbations.

**Adversarial training as a defense.** The adversarial training procedure which feeds adversarially perturbed examples back into the training data is widely regarded as one of the most successful method to train robust deep neural networks. Its classical version detailed by Madry et al. (2018) has been augmented in different ways – with changes in the attack procedure (e.g., by incorporating momentum; Dong et al., 2018), loss function (e.g., logit pairing; Mosbach et al., 2018) or model architecture (e.g., feature denoising; Xie et al., 2019). Other notable works include the work by Zhang et al. (2019) who proposed TRADES which balances the trade-off between standard and robust accuracy, and the work by Wang et al. (2020) who proposed MART which also addresses this trade-off by using boosted loss functions. Both works achieved state-of-the-art performance against  $\ell_\infty$  norm-bounded perturbations on CIFAR-10. The work from Rice et al. (2020) stood out as a study on robust overfitting which demonstrated that improvements similar to TRADES and MART could be obtained more easily using classical adversarial training with early stopping. This study revealed that there is much we do not yet understand about adversarial training, and serves as one of our motivations for performing a holistic analysis of different aspects of adversarial training. So far, to the best of our knowledge, there has been no systematic study of adversarial training.

**Other defenses.** Many other alternative defenses are not covered in the scope of this paper. They range from preprocessing techniques (Buckman et al., 2018; Guo et al., 2018) to detection algorithms (Feinman et al., 2017; Metzen et al., 2017), and also include the definition of new regularizers (Moosavi-Dezfooli et al., 2019; Qin et al., 2019; Xiao et al., 2019). The difficulty of adversarial evaluation also drove the need for *certified defenses* (Cohen et al., 2019; Gowal et al., 2019a; Mirman et al., 2018; Salman et al., 2019; Wong et al., 2018; Zhang et al., 2020), but the guarantees that these techniques provide do not yet match the empirical robustness obtained through adversarial training.

**Adversarial evaluation.** It is worth noting that many of the defense strategies proposed in the literature (Kannan et al., 2018; Lu et al., 2017; Papernot et al., 2016; Tao et al., 2018; Zhang & Wang, 2019) were broken by stronger adversaries (Athalye & Sutskever, 2018; Athalye et al., 2018; Carlini, 2019; Carlini & Wagner, 2016, 2017b; Engstrom et al., 2018; Uesato et al., 2018). Hence, the robust accuracy obtained under different evaluation protocols cannot be easily compared and care has to be taken to make sure the evaluation is as strong as is possible (Carlini et al., 2019). In this manuscript, we evaluate

each model against two of the strongest adversarial attacks, `AUTOATTACK` and `MULTITARGETED`, developed by [Croce & Hein \(2020\)](#) and [Gowal et al. \(2019b\)](#), respectively.

## 2.2. Adversarial training

[Madry et al. \(2018\)](#) formulate a saddle point problem whose goal is to find model parameters  $\theta$  that minimize the adversarial risk:

$$\underbrace{\arg \min_{\theta} \mathbb{E}_{(x,y) \sim \mathcal{D}}}_{\text{outer minimization}} \underbrace{\left[ \max_{\delta \in \mathbb{S}} l(f(x + \delta; \theta), y) \right]}_{\text{inner maximization}} \quad (1)$$

where  $\mathcal{D}$  is a data distribution over pairs of examples  $x$  and corresponding labels  $y$ ,  $f(\cdot; \theta)$  is a model parametrized by  $\theta$ ,  $l$  is a suitable loss function (such as the 0 – 1 loss in the context of classification tasks), and  $\mathbb{S}$  defines the set of allowed perturbations (i.e., the adversarial input set or threat model). For  $\ell_p$  norm-bounded perturbations of size  $\epsilon$ , the adversarial set is defined as  $\mathbb{S}_p = \{\delta \mid \|\delta\|_p < \epsilon\}$ . Hence, for  $\ell_\infty$  norm-bounded perturbations  $\mathbb{S} = \mathbb{S}_\infty$  and for  $\ell_2$  norm-bounded perturbations  $\mathbb{S} = \mathbb{S}_2$

**Inner maximization.** As finding the optimum of the inner maximization problem is NP-hard, several methods (also known as “attacks”) have been proposed to approximate its solution. [Madry et al. \(2018\)](#) use PGD,<sup>2</sup> which replaces the non-differentiable 0 – 1 loss  $l$  with the cross-entropy loss  $l_{\text{xent}}$  and computes an adversarial perturbation  $\hat{\delta} = \delta^{(K)}$  in  $K$  gradient ascent steps of size  $\alpha$  as

$$\delta^{(k+1)} \leftarrow \text{proj}_{\mathbb{S}} \left( \delta^{(k)} + \alpha \text{sign} \left( \nabla_{\delta^{(k)}} l_{\text{xent}}(f(x + \delta^{(k)}; \theta), y) \right) \right) \quad (2)$$

where  $\delta^{(0)}$  is chosen at random within  $\mathbb{S}$ , and where  $\text{proj}_{\mathbb{A}}(\mathbf{a})$  projects a point  $\mathbf{a}$  back onto a set  $\mathbb{A}$ ,  $\text{proj}_{\mathbb{A}}(\mathbf{a}) = \text{argmin}_{\mathbf{a}' \in \mathbb{A}} \|\mathbf{a} - \mathbf{a}'\|_2$ . We will refer to this inner optimization procedure with  $K$  steps as  $\text{PGD}^K$ .

**Outer minimization.** For each example  $x$  with label  $y$ , adversarial training minimizes the loss given by

$$\mathcal{L}_{\theta}^{\text{AT}} = l_{\text{xent}}(f(x + \hat{\delta}; \theta), y) \approx \max_{\delta \in \mathbb{S}} l_{\text{xent}}(f(x + \delta; \theta), y) \quad (3)$$

where  $\hat{\delta}$  is given by [Equation 2](#) and  $l_{\text{xent}}$  is the softmax cross-entropy loss.

## 3. Setup and implementation details

Initially, we focus on robustness to  $\ell_\infty$  norm-bounded perturbations on `CIFAR-10` of size  $\epsilon = 8/255$ . [section 5](#) combines individual components to surpass the state-of-the-art and tests their generality against other datasets (i.e., `CIFAR-100` and `MNIST`) and another threat model (i.e.,  $\ell_2$  norm-bounded perturbations of size  $\epsilon = 128/255$ ). First, we describe the experimental setup.

<sup>2</sup>There exists a few variants of PGD which normalize the gradient step differently (e.g., using an  $\ell_2$  normalization for  $\ell_2$  norm-bounded perturbations).

### 3.1. Setup

**Architecture.** For consistency with prior work on adversarial robustness (Madry et al., 2018; Rice et al., 2020; Uesato et al., 2019; Zhang et al., 2019), we use Wide ResNets (WRNs) (He et al., 2016; Zagoruyko & Komodakis, 2016). Our baseline model (on which most experiments are performed) is 28 layers deep with a width multiplier of 10, and is denoted by WRN-28-10. We also use deeper (up to 70 layers) and wider (up to 20) models. Our largest model is a WRN-70-16 containing 267M parameters, our smallest model is a WRN-28-10 containing 36M parameters. A popular option in the literature is the WRN-34-20, which contains 186M parameters.

**Outer minimization.** We use Stochastic Gradient Descent (SGD) with Nesterov momentum (Nesterov, 1983; Polyak, 1964). The initial learning rate of 0.1 is decayed by  $10\times$  half-way and three-quarters-of-the-way through training (we refer to this schedule as the *multistep* schedule). We use a global weight decay parameter of  $5 \times 10^{-4}$ . In the basic setting without additional unlabeled data, we use a batch size of 128 and train for 200 epochs (i.e., 78K steps). With additional unlabeled data, we use a batch size of 1024 with 512 samples from CIFAR-10 and 512 samples from a subset of 500K images extracted from the tiny images dataset 80M-TI (Torralba et al., 2008)<sup>3</sup> and train for 19.5K steps (i.e., 400 CIFAR-10-equivalent epochs). To use the unlabeled data with adversarial training, we use the *pseudo-labeling* mechanism presented by Carmon et al. (2019): a separate non-robust classifier is trained on clean data from CIFAR-10 to provide labels to the unlabeled samples (the dataset created by Carmon et al., 2019 is already annotated with such labels). Our batches are split over 32 Google Cloud TPU v3 cores. As is common on CIFAR-10, we augment our samples with random crops (i.e., pad by 4 pixels and crop back to  $32 \times 32$ ) and random horizontal flips.

**Inner maximization.** The inner maximization in Equation 3 is implemented using PGD<sup>10</sup>.<sup>4</sup> We used a step-size  $\alpha$  of  $2/255$  and  $15/255$  for  $\ell_\infty$  and  $\ell_2$  norm-bounded perturbations, respectively. With this setup, training without additional data takes approximately 1 hour and 30 minutes for a WRN-28-10 (peak accuracy as measured on a validation set disjoint from the test set is obtained after 1 hour and 15 minutes; for a WRN-70-16 peak accuracy is obtained after 4 hours). With additional unlabeled data, training takes approximately 2 hours.

**Evaluation protocol.** As adversarial training is a bit more noisy than regular training, for each hyperparameter setting, we train two models. Throughout training we measure the robust accuracy using PGD<sup>40</sup> on 1024 samples from a separate validation set (disjoint from the training and test set). Similarly to Rice et al. (2020), we perform early stopping by keeping track of model parameters that achieve the highest robust accuracy (i.e., lowest adversarial risk as shown in Equation 1) on the validation set. From both models, we pick the one with highest robust accuracy on the validation set and use this model for a further more thorough evaluation. Finally, the robust accuracy is reported on the full test set against a mixture of AUTOATTACK (Croce & Hein, 2020) and MULTITARGETED (Gowal et al., 2019b). We execute the following sequence of attacks: AUTOPGD on the cross-entropy loss with 5 restarts and 100 steps, AUTOPGD on the difference of logits ratio loss with 5 restarts and 100 steps, MULTITARGETED on the margin loss with 10 restarts and 200 steps.<sup>5</sup> We also report the clean accuracy which is the top-1 accuracy without adversarial perturbations.

<sup>3</sup>We use the dataset from Carmon et al. (2019) available at <https://github.com/yaircarmon/semisup-adv>.

<sup>4</sup>Unless special care is taken (Wong et al., 2020), using less than 7 steps often results in gradient obfuscated models (Qin et al., 2019), using more steps did not provide significant improvements in our experiments

<sup>5</sup>For reference, the AUTOATTACK leaderboard at <https://github.com/fra31/auto-attack> evaluates the model from Rice et al. (2020) to 53.42%, while this evaluation computes a robust accuracy of 53.38% for the same model. The AUTOATTACK leaderboard also evaluates the model from Carmon et al. (2019) to 59.53%, while this evaluation computes a robust accuracy of 59.47% for the same model.

### 3.2. Baseline.

As a comparison point, we train a WRN-28-10 ten times with the default settings given above for both the CIFAR-10-only and the additional data settings. The resulting robust accuracy on the test set is  $50.80 \pm 0.23\%$  (for CIFAR-10-only) and  $58.41 \pm 0.25\%$  (with additional unlabeled data). When using a WRN-34-20, we obtain 52.91% which is in line with the model obtained by Rice et al. (2020) for the same settings (i.e., 53.38%). When using TRADES (instead of regular adversarial training) in the additional data setting, we obtain 59.45% which is in line with the model obtain by Carmon et al. (2019) for the same settings (i.e., 59.47%). As our pipeline is implemented in JAX (Bradbury et al., 2018) and Haiku (Hennigan et al., 2020), we do not exclude some slight differences in data preprocessing and network initialization.

## 4. Experiments and analysis

The following sections detail different independent experiments (more experiments are available in the appendix). Each section is self-contained to allow the reader to jump to any section of interest. The outline is as follows:

4.1	Losses for Outer minimization . . . . .	6
4.2	Inner maximization . . . . .	7
4.2.1	Inner maximization loss . . . . .	7
4.2.2	Inner maximization perturbation radius . . . . .	8
4.3	Additional unlabeled data . . . . .	9
4.3.1	Quality and quantity . . . . .	9
4.3.2	Ratio of labeled-to-unlabelled data per batch . . . . .	10
4.4	Effects of scale . . . . .	11
4.5	Other tricks . . . . .	11
4.5.1	Model weight averaging . . . . .	11
4.5.2	Activation functions . . . . .	12

### 4.1. Losses for Outer minimization

As explained in subsection 2.2, adversarial training as proposed by Madry et al. (2018) aims to minimize the loss given in Equation 3 and is usually implemented as

$$\mathcal{L}_\theta^{\text{AT}} = l_{\text{xent}}(f(\mathbf{x} + \hat{\boldsymbol{\delta}}; \boldsymbol{\theta}), y), \quad \text{where } \hat{\boldsymbol{\delta}} \approx \arg \max_{\boldsymbol{\delta} \in \mathbb{S}} l_{\text{xent}}(f(\mathbf{x} + \boldsymbol{\delta}; \boldsymbol{\theta}), y). \quad (4)$$

Here,  $l_{\text{xent}}$  denotes the cross-entropy loss and  $\hat{\boldsymbol{\delta}}$  is treated as a constant (i.e., there is no back-propagation through the inner optimization procedure). One of most successful variant of adversarial training is TRADES (Zhang et al., 2019) which derives a theoretically grounded regularizer that balances the trade-off between standard and robust accuracy. The overall loss used by TRADES is given by

$$\mathcal{L}_\theta^{\text{TRADES}} = l_{\text{xent}}(f(\mathbf{x}; \boldsymbol{\theta}), y) + \beta \max_{\boldsymbol{\delta} \in \mathbb{S}} D_{\text{KL}}(f(\mathbf{x} + \boldsymbol{\delta}; \boldsymbol{\theta}), f(\mathbf{x}; \boldsymbol{\theta})), \quad (5)$$

where  $D_{\text{KL}}$  denotes the Kullback-Leibler divergence. TRADES is one of the core components used by Carmon et al. (2019) within RST and by Uesato et al. (2018) within UAT-OT. A follow-up work (Wang et al., 2020), known as Misclassification Aware Adversarial Training (MART), introduced a boosted loss that differentiates between the misclassified and correctly classified examples in a bid to improve this trade-off further. We invite the reader to refer to Wang et al. (2020) for more details.

Table 1 | Clean (without perturbations) and robust (under adversarial attack) accuracy obtained by Adversarial Training (AT), TRADES and MART trained on CIFAR-10 (with and without additional unlabeled data) against  $\ell_\infty$  norm-bounded perturbations of size  $\epsilon = 8/255$ .

SETUP	CIFAR-10		with 80M-Ti	
	CLEAN	ROBUST	CLEAN	ROBUST
AT (Madry et al., 2018)	84.85±1.20%	50.80±0.23%	90.93±0.25%	58.41±0.25%
TRADES (Zhang et al., 2019)	82.74%	51.91%	88.36%	59.45%
MART (Wang et al., 2020)	80.51%	51.93%	90.45%	58.25%

**Results.** Table 1 shows the performance of TRADES and MART compared to adversarial training (AT). We observe that while TRADES systematically improves upon AT in both data settings, this is not the case for MART. We find that MART has the propensity to create moderate forms of gradient masking against weak attacks like PGD<sup>20</sup>. In one extreme case, a WRN-70-16 trained with additional unlabeled data using MART obtained an accuracy of 71.08% against PGD<sup>20</sup> which dropped to 60.63% against our stronger suite of attacks (this finding is consistent with the AutoAttack leaderboard at <https://github.com/fra31/auto-attack>).

**Key takeaways.** Contrary to the suggestion of Rice et al. (2020) (i.e., “the original PGD-based adversarial training method can actually achieve the same robust performance as state-of-the-art method”, see subsection 2.1), TRADES (when combined with early-stopping – as our setup dictates) is more competitive than classical adversarial training. The results also highlight the importance of strong evaluations beyond PGD<sup>20</sup> (including evaluations of the validation set used for early stopping).

## 4.2. Inner maximization

### 4.2.1. Inner maximization loss

Most works use the same loss (e.g., cross-entropy loss or Kullback-Leibler divergence) for solving the inner maximization problem (i.e., finding an adversarial example) and the outer minimization problem (i.e., training the neural network). However, there are many plausible approximations for the inner maximization. For example, instead of using the cross-entropy loss or Kullback-Leibler divergence for the inner maximization, Uesato et al. (2018) used the margin loss  $\max_{i \neq y} f(\mathbf{x}; \theta)_i - f(\mathbf{x}; \theta)_y$  which improved attack convergence speed. Similarly, we could mix the cross-entropy loss with TRADES via the following:

$$\begin{aligned} \mathcal{L}_\theta^{\text{TRADES-XENT}} &= l_{\text{xent}}(f(\mathbf{x}; \theta), y) + \beta D_{\text{KL}}(f(\mathbf{x} + \hat{\delta}; \theta), f(\mathbf{x}; \theta)) \text{ where} \\ \hat{\delta} &\approx \arg \max_{\delta \in \mathbb{S}} l_{\text{xent}}(f(\mathbf{x} + \delta; \theta), y). \end{aligned} \quad (6)$$

Or mix the Kullback-Leibler divergence with classical adversarial training:

$$\mathcal{L}_\theta^{\text{AT-KL}} = l_{\text{xent}}(f(\mathbf{x} + \hat{\delta}; \theta), y) \text{ where } \hat{\delta} \approx \arg \max_{\delta \in \mathbb{S}} D_{\text{KL}}(f(\mathbf{x} + \delta; \theta), f(\mathbf{x}; \theta)). \quad (7)$$

Below are our observations on the effects of robustness and clean accuracy when we combine different inner and outer optimisation losses.

**Results.** Table 2 shows the performance of different inner and outer loss combinations. Each combination is evaluated against two adversaries: a weaker PGD<sup>40</sup> attack using the margin loss (and denoted by

Table 2 | Clean (without perturbations) and robust (under adversarial attack) accuracy obtained by TRADES and Adversarial Training (AT) with different inner losses trained on CIFAR-10 (with and without additional unlabeled data) against  $\ell_\infty$  norm-bounded perturbations of size  $\epsilon = 8/255$ . The robust accuracy is measured using  $\text{PGD}_{\text{margin}}^{40}$  with a margin loss ( $\text{PGD}_{\text{margin}}^{40}$ ) and our combination of AUTOATTACK and MULTITARGETED (AA+MT).

SETUP	CIFAR-10			with 80M-T1		
	CLEAN	$\text{PGD}_{\text{margin}}^{40}$	AA+MT	CLEAN	$\text{PGD}_{\text{margin}}^{40}$	AA+MT
AT-XENT (Madry et al., 2018)	84.85%	53.87%	50.80%	90.93%	61.46%	58.41%
AT-KL	88.21%	50.67%	48.53%	91.86%	59.49%	56.89%
AT-MARGIN	85.12%	<b>54.72%</b>	48.79%	90.01%	<b>61.53%</b>	55.18%
TRADES-XENT	83.01%	54.19%	<b>52.76%</b>	89.12%	61.25%	58.98%
TRADES-KL (Zhang et al., 2019)	82.74%	53.85%	51.91%	88.36%	61.11%	<b>59.45%</b>
TRADES-MARGIN	81.60%	54.47%	51.28%	86.88%	61.37%	57.82%

$\text{PGD}_{\text{margin}}^{40}$ ) and our stronger combination of attacks (as detailed in subsection 3.1 and denoted AA+MT). The first observation is that TRADES obtains higher robust accuracy compared to classical adversarial training (AT) across most combinations of inner losses. We note that the clean accuracy is higher for AT compared to TRADES and address this trade-off in the next section (subsubsection 4.2.2). In the low-data setting, the combination of TRADES with cross-entropy (TRADES-XENT) yields the best robust accuracy. In the high-data setting, we obtain higher robust accuracy using TRADES-KL.

Our second observation is that using margin loss during training can show signs of gradient masking: models trained using margin loss show higher degradation in robust accuracy when evaluated against the stronger adversary (AA+MT) as opposed to the weaker  $\text{PGD}_{\text{margin}}^{40}$ . Table 2 shows that the drop in robust accuracy can be as high as -6.35%.<sup>6</sup> This level of gradient masking is most prominent in AT-MARGIN and is mitigated when we use TRADES for the outer minimization. This degradation in robust accuracy is significantly reduced when we use cross-entropy as the inner maximization loss.

**Key takeaways.** Similarly to the observation made in subsection 4.1, TRADES obtains higher adversarial accuracy compared to classical adversarial training. We found that using margin loss during training (for the inner maximization procedure) creates noticeable gradient masking.

#### 4.2.2. Inner maximization perturbation radius

Several works explored the use of larger (Gowal et al., 2019a) or adaptive (Balaji et al., 2019) perturbation radii. Like TRADES, using different perturbation radii is an attempt to bias the clean to robust accuracy trade-off: as we increase the training perturbation radius we expect increased robustness and lower clean accuracy.

**Results.** Table 3 shows the effect of increasing the perturbation radius  $\epsilon$  by a factor 1.1 $\times$  and 1.2 $\times$  the original value of 8/255 (during training, not during evaluation). We notice that adversarial training (AT) can close the gap to TRADES as we increase the perturbation radius (especially in the low-data regime). Although not reported here, we noticed that TRADES does not get similar improvements in performance with larger radii (possibly because TRADES is already actively managing the trade-off with clean accuracy).

<sup>6</sup>Using margin loss for evaluation is not uncommon, since it has been suggested to yield a stronger adversary (see Carlini & Wagner, 2017b; Liu et al., 2017).



Table 3 | Clean (without perturbations) and robust (under adversarial attack) accuracy obtained on CIFAR-10 (with and without additional unlabeled data) against  $\ell_\infty$  norm-bounded perturbations of size  $\epsilon = 8/255$  when using different perturbation radii for the inner maximization trained.

SETUP	CIFAR-10		with 80M-TI	
	CLEAN	ROBUST	CLEAN	ROBUST
AT $\epsilon = 8/255$ (Madry et al., 2018)	84.85±1.20%	50.80±0.23%	90.93±0.25%	58.41±0.25%
AT $\epsilon = 8.8/255$	82.13%	51.65%	90.16%	58.72%
AT $\epsilon = 9.6/255$	83.60%	51.81%	89.39%	58.77%
TRADES $\epsilon = 8/255$ (Zhang et al., 2019)	82.74%	51.91%	88.36%	59.45%

**Key takeaways.** Tuning the training perturbation radius can marginally improve robustness (when using classical adversarial training). We posit that understanding when and how to use larger perturbation radii might be critical towards our understanding of robust generalization. Work from Balaji et al. (2019) do provide additional insights, but the topic remains largely under-explored.

### 4.3. Additional unlabeled data

After the work from Schmidt et al. (2018) which posits that robust generalization requires more data, Hendrycks et al. (2019) demonstrated that one could leverage additional labeled data from IMAGENET to improve the robust accuracy of models on CIFAR-10. Uesato et al. (2019) and Carmon et al. (2019) were among the first to introduce additional unlabeled data to CIFAR-10 by extracting images from 80M-TI (i.e., subset of high scoring images from a CIFAR-10 classifier). Uesato et al. (2019) used 200K additional images to train their best model as they observed that using more data (i.e., 500K images) worsen their results. This suggests that additional data needs to be close enough to the original CIFAR-10 images to be useful. This is something already suggested by Oliver et al. (2018) in the context of semi-supervised learning.

#### 4.3.1. Quality and quantity

In this experiment, we use four different subsets of additional unlabeled images extracted from 80M-TI. The first set with 500K images is the additional data used by Carmon et al. (2019).<sup>7</sup> The second, third and fourth sets consist of 200K, 500K and 1M images regenerated using a process identical to Carmon et al. (2019) with a another pre-trained classifier (achieving 95.86% accuracy on the test set). To generate a dataset of size  $N$ , we remove duplicates from the CIFAR-10 test set, score the remaining images using a standard CIFAR-10 classifier, and pick the top- $N/10$  scoring images from each class. Hence, the dataset with 500K images contains all the images from the dataset with 200K images and, similarly, the dataset with 1M images contains all the images from the dataset with 500K images. As the datasets increase in size, the images they contain may become less relevant to the CIFAR-10 classification task (as their standard classifier score becomes smaller).

**Results.** Table 4 shows the performance of adversarial training with *pseudo-labeling* as the quantity of additional unlabeled data increases. This training scheme is identical to UAT-FT (as introduced by Uesato et al., 2019) and is slightly different to the one proposed in Carmon et al. (2019) (which used TRADES).

Table 4 | Accuracy under  $\ell_\infty$  attacks of size  $\epsilon = 8/255$  on CIFAR-10 as the quantity of unlabeled data increases.

QUANTITY	CLEAN	ROBUST
500K (Carmon et al., 2019)	90.93%	58.41%
200K (regenerated)	90.95%	57.29%
500K (regenerated)	90.68%	59.12%
1M (regenerated)	91.00%	58.89%

<sup>7</sup><https://github.com/yaircarmon/semisup-adv>

Firstly, we note that our regenerated set of 500K images improves robustness (+0.71%) compared to [Carmon et al. \(2019\)](#). Secondly, similar to the observations made by [Uesato et al. \(2019\)](#), there is a sweet spot where additional data is maximally useful. Going from 200K to 500K additional images improves robust accuracy by +1.83%. However, increasing the amount of additional images further to 1M is detrimental (-0.23%). This suggests that more data improves robustness as long as the additional images relate to the original CIFAR-10 dataset (e.g., the more images we extract, the less likely it is that these images correspond to classes within CIFAR-10).

**Key takeaways.** Small differences (e.g., different classifiers used for *pseudo-labeling*) in the process that extracts additional unlabeled data can have significant impact on robustness (i.e., models trained on our regenerated dataset obtain higher robust accuracy than those trained with the data from [Carmon et al., 2019](#)). There is also a trade-off between the quantity and the quality of the extra unlabeled data (i.e., increasing the amount of unlabeled data to 1M did not increase robustness).

#### 4.3.2. Ratio of labeled-to-unlabelled data per batch

In this section, all the experiments use the unlabeled data from [Carmon et al. \(2019\)](#). In the baseline setting, as done in [Carmon et al. \(2019\)](#), each batch during training uses 50% labeled data and the rest for unlabeled data. This effectively downweights unlabeled images by a factor 10 $\times$ , as we have 50K labeled images and 500K unlabeled images. Increasing this ratio reduces the weight given to additional data and puts more emphasis of the original CIFAR-10 images.

**Results.** [Figure 2](#) shows the robust accuracy as we vary that ratio. We observe that giving slightly more importance to unlabeled data helps. More concretely, we find an optimal ratio of labeled-to-unlabeled data of 3:7, which provides a boost of +0.95% over the 1:1 ratio. This suggest that the additional data extracted by [Carmon et al. \(2019\)](#) is well aligned with the original CIFAR-10 data and that we can improve robust generalization by allowing the model to see this additional data more frequently. Increasing this ratio (i.e., reducing the importance of the unlabeled data) gradually degrades robustness and, eventually, the robust accuracy matches the one obtained by models trained without additional data.

We also experimented with label smoothing (for both labeled and unlabeled data independently). Label smoothing should counteract the effect of the noisy labels resulting from the classifier used in the *pseudo-labeling* process. However, we did not observe improvements in performance for any of the settings tried.

**Key takeaways.** Tuning the weight given to unlabeled examples (by varying the labeled-to-unlabeled data ratio per batch) can provide improvements in robustness. This experiment highlight that a careful treatment of the extra unlabeled data can provide improvements in adversarial robustness.

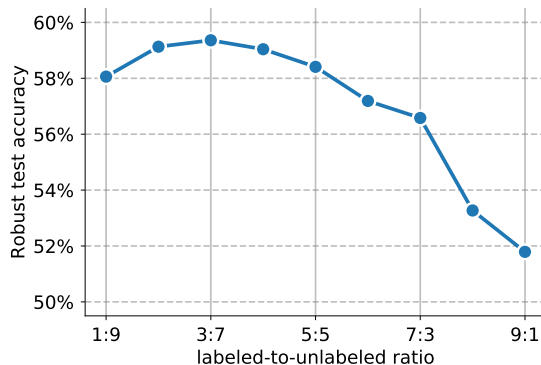
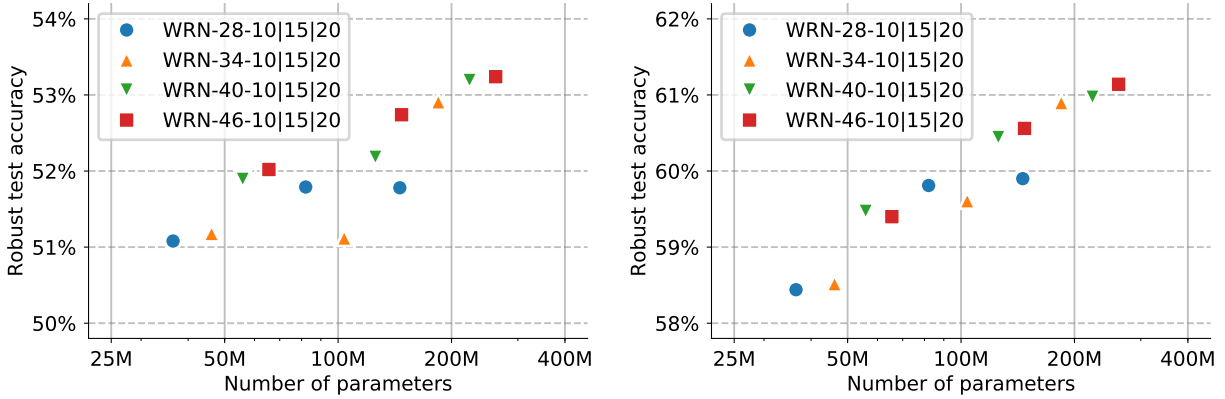


Figure 2 | Accuracy under  $\ell_\infty$  attacks of size  $\epsilon = 8/255$  on CIFAR-10 as we vary the ratio of labeled-to-unlabeled data.



(a) CIFAR-10

(b) CIFAR-10 and 80M-TI

Figure 3 | Clean accuracy and accuracy under  $\ell_\infty$  attacks of size  $\epsilon = 8/255$  on CIFAR-10 as the network architecture changes. Panel a restricts the available data to CIFAR-10, while panel b uses 500K additional unlabeled images extracted from 80M-TI.

#### 4.4. Effects of scale

Rice et al. (2020) observed that increasing the model width improves robust accuracy despite the phenomenon of robust overfitting (which favors the use of early stopping in adversarial training). Uesato et al. (2019) also trialed deeper models with a WRN-106-8 and observed improved robustness. A most systematic study of the effect of network depth was also conducted by Xie & Yuille (2020) on IMAGENET (scaling a ResNet to 638 layers). However, there have not been any controlled experiments on CIFAR-10 that varied both depth and width of WRNs. We note that most work on adversarial robustness on CIFAR-10 use either a WRN-34-10 or a WRN-28-10 network, with WRN-34-20 being another popular option.

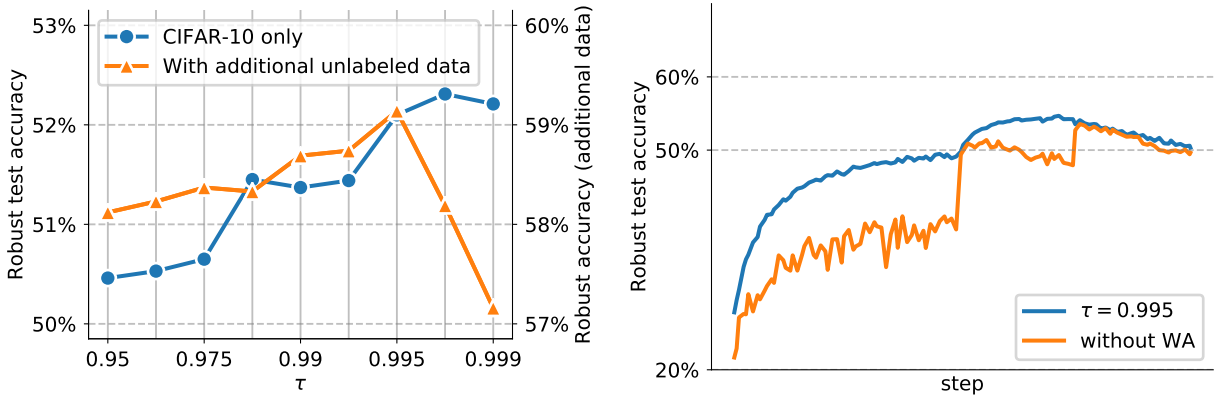
**Results.** Figure 3 shows the effect of increasing the depth and width of our baseline network. It is possible to observe that, while both depth and width increase the number of effective model parameters, they do not always provide the same effect on robustness. For example, a WRN-46-15 which trains in roughly the same time as a WRN-28-20 (about 5 hours in our setup) reaches higher robust accuracy: +0.96% and +0.66% on the settings without and with additional data, respectively. Table 14 in the appendix also shows that the clean accuracy improves as networks become larger.

**Key takeaways.** Larger models provide improved robustness (Madry et al., 2018; Uesato et al., 2019; Xie & Yuille, 2019) and, for identical parameter count, deeper models can perform better.

#### 4.5. Other tricks

##### 4.5.1. Model weight averaging

Model Weight Averaging (WA) (Izmailov et al., 2018) is widely used in classical training (Tan & Le, 2019), and leads to better generalization. The WA procedure finds much flatter solutions than SGD, and approximates ensembling with a single model. To the best of our knowledge, the effect of WA on robustness have not been studied in the literature. Ensembling has received some attention (Pang et al., 2019; Strauss et al., 2017), but requires training multiple models. We implement WA using an exponential moving average  $\theta'$  of the model parameters  $\theta$  with a decay rate  $\tau$ : we execute  $\theta' \leftarrow \tau \cdot \theta' + (1 - \tau) \cdot \theta$



(a) Final robust accuracy

(b) Robust accuracy during training (PGD<sup>40</sup>)

Figure 4 | Accuracy under  $\ell_\infty$  attacks of size  $\epsilon = 8/255$  on CIFAR-10 when using model weight averaging (WA). Panel a shows the final robust accuracy obtained for different values of the decay rate  $\tau$  for the settings without (blue and left y-axis) and with additional unlabeled data (orange and right y-axis). Panel b shows the evolution of the robust accuracy as training progresses.

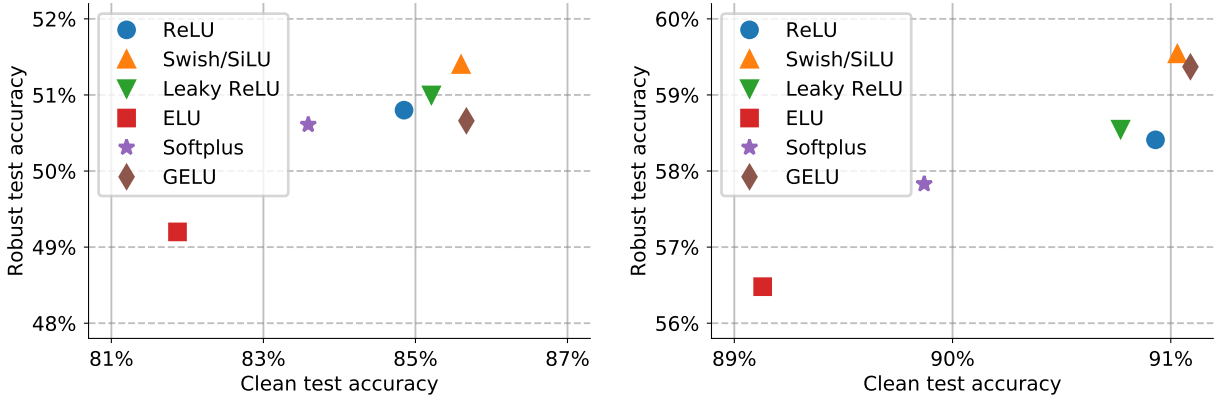
at each training step. During evaluation, the weighted parameters  $\theta'$  are used instead of the trained parameters  $\theta$ .

**Results.** Figure 4 summarizes the performance of model weight averaging (detailed results are in Table 15 in the appendix). Panel 4a demonstrates significant improvements in robustness: +1.41% and +0.73% with respect to the baseline without WA for settings without and with additional data, respectively. In fact, in the low-data regime, WA provides an improvement similar to that of TRADES (+1.11%). A possible explanation for this phenomena is possibly given by panel 4b. We observe that not only that WA achieves higher robust accuracy, but also that it maintains this higher accuracy over a few training epochs (about 25 epochs). This reduces the sensitivity to early stopping which may miss the most robust checkpoint (happening shortly after the second learning rate decay). Another important benefit of WA is its rapid convergence to about 50% robust accuracy (against PGD<sup>40</sup>) in the early stages of training, which suggests that it could be combined with efficient adversarial training techniques such as the one presented by Wong et al. (2020).

**Key takeaways.** Although widely used for standard training, WA has not been explored within adversarial training. We discover that WA provides sizeable improvements in robustness and hope that future work can explore this phenomenon.

#### 4.5.2. Activation functions

With the exception from work by Xie et al. (2020a) which focused on IMAGENET, there have been little to no investigations into the effect of different activation functions on adversarial training. Xie et al. (2020a) discovered that “smooth” activation functions yielded higher robustness when using weak adversaries during training (PGD with a low number of steps). In particular, they posit that they allow adversarial training to find harder adversarial examples and compute better gradient updates. Qin et al. (2019) also experimented with softplus activations with success.



(a) CIFAR-10

(b) CIFAR-10 and 80M-Ti

Figure 5 | Clean accuracy and accuracy under  $\ell_\infty$  attacks of size  $\epsilon = 8/255$  on CIFAR-10 for different activation functions. Panel a restricts the available data to CIFAR-10, while panel b uses 500K additional unlabeled images extracted from 80M-Ti.

**Results.** While we observe in Figure 5 that activation functions other than ReLU (Nair & Hinton, 2010) can positively affect clean and robust accuracy, the trend is not as clear as the one observed by Xie et al. (2020a) on IMAGENET. In fact, apart from Swish/SiLU (Elfwing et al., 2018; Hendrycks & Gimpel, 2016; Ramachandran et al., 2017), which provides improvements of +0.8% and +1.13% in the settings without and with additional unlabeled data, the order of the best performing activation functions changes when we go from the CIFAR-10-only setting to the setting with additional unlabeled data. Overall, ReLU remains a good choice.

**Key takeaways.** The choice of activation function matters: we found that while Swish/SiLU performs best in our experiments. Other “smooth” activation functions (Xie et al., 2020b) do not necessarily correlate positively with robustness in our experiments.

## 5. A new state-of-the-art

To evaluate the combined effects of our findings, we train a single model according to the key takeaways from each section. We hope that this exercise can provide valuable insights. In particular, we combine the following elements: (i) TRADES as detailed by Zhang et al. (2019), (ii) model weight averaging with  $\tau = 0.995$  (per 1024 examples), (iii) a larger model with a WRN-70-16 (we also evaluate smaller models on CIFAR-10 against  $\ell_\infty$  norm-bounded perturbations), (iv) Swish/SiLU activations. In the setting without additional labeled data, we use the *multistep* learning rate schedule (as detailed in subsection 3.1) with a batch size of 512 (the effective weight averaging decay  $\tau$  is set to  $\sqrt{0.995}$ ). In the setting with additional labeled data, we preferred the *cosine* decay learning rate schedule (Loshchilov & Hutter, 2017) without restarts (which was better than *multistep* when the model size increased beyond WRN-28-10). We also used a labeled-to-unlabeled ratio of 3:7.

Table 5 shows the results as well as the known state-of-the-art. We evaluate robust accuracy using the AUTOATTACK pipeline available from <https://github.com/fra31/auto-attack> and denoted AA, and using our combined set of attacks denoted AA+MT and described in subsection 3.1. On CIFAR-10 against  $\ell_\infty$  norm-bounded perturbations of size  $\epsilon = 8/255$ , we improve state-of-the-art robust accuracy by +3.46% and +6.35% without and with additional data, respectively. At equal model size, we improve robust accuracy by +3.12% and +3.27%, respectively. Most notably, without additional data, we improve on

the results of four methods that used additional data (Hendrycks et al., 2019; Sehwan et al., 2020; Uesato et al., 2019; Wang et al., 2020). With additional data, we surpass the barrier of 60% for the first time.

To test the generality of our findings, we keep the same hyper-parameters and train adversarially robust models on CIFAR-10 against  $\ell_2$  norm-bounded perturbations of size  $\epsilon = 128/255$  and on CIFAR-100 against  $\ell_\infty$  norm-bounded perturbations of size  $\epsilon = 8/255$ .<sup>8</sup> In the four cases (with and without additional data), we surpass the known state-of-the-art by significant margins.<sup>9</sup>

## 6. Conclusion

In this work, we performed a systematic analysis of many different aspects surrounding adversarial training that can affect the robustness of trained networks. The goal was to see how far we could push robust accuracy through adversarial training with the right combination of network size, activation functions, additional data and model weight averaging. We find that by combining these different factors carefully we can achieve robust accuracy that improves upon the state-of-the-art by more than 6% (in the setting using additional data on CIFAR-10 against  $\ell_\infty$  norm-bounded perturbations of size  $\epsilon = 8/255$ ). We hope that this work can serve as a reference point for the current state of adversarial robustness and can help others build new techniques that can ultimately reach higher adversarial robustness.

<sup>8</sup>For CIFAR-100, we extract new additional unlabeled data by excluding images from its test set.

<sup>9</sup>For completeness, we also include results on MNIST and SVHN.

Table 5 | Clean (without perturbations) and robust (under adversarial attack) accuracy obtained by different setups (with and without additional unlabeled data). The accuracies are reported on full test sets. \* Trained by us using standard adversarial training with early stopping.

MODEL	DATASET	NORM	RADIUS	CLEAN	PGD <sup>40</sup>	AA+MT	AA
<b>WITHOUT 80M-TI</b>							
Pang et al. (2020b) (WRN-34-20)				85.14%	–	–	53.74%
Ours (WRN-70-16)	CIFAR-10	$\ell_\infty$	$\epsilon = 8/255$	85.29%	58.22%	57.14%	<b>57.20%</b>
Ours (WRN-34-20)				85.64%	57.73%	56.82%	56.86%
Engstrom et al. (2019) (ResNet-50)				90.83%	–	–	69.24%
Ours (WRN-70-16)	CIFAR-10	$\ell_2$	$\epsilon = 128/255$	90.90%	75.41%	74.45%	<b>74.50%</b>
Rice et al. (2020) (ResNet-18)				53.83%	–	–	18.95%
Ours (WRN-70-16)	CIFAR-100	$\ell_\infty$	$\epsilon = 8/255$	60.86%	31.47%	30.67%	<b>30.03%</b>
Zhang et al. (2020) (7-layer CNN)				98.38%	–	–	93.96%
Ours (WRN-28-10)	MNIST	$\ell_\infty$	$\epsilon = 0.3$	99.26%	97.27%	96.38%	<b>96.34%</b>
Rice et al. (2020) (WRN-28-10)*				92.15%	57.82%	50.08%	–
Ours (WRN-34-20)	SVHN	$\ell_\infty$	$\epsilon = 8/255$	93.13%	61.12%	<b>58.02%</b>	–
Ours (WRN-28-10)				92.87%	60.17%	56.83%	–
<b>WITH ADDITIONAL UNLABELED DATA FROM 80M-TI</b>							
Carmon et al. (2019) (WRN-28-10)				89.69%	–	59.47%	59.53%
Ours (WRN-70-16)				91.10%	67.16%	65.87%	<b>65.88%</b>
Ours (data from Carmon et al., 2019)	CIFAR-10	$\ell_\infty$	$\epsilon = 8/255$	90.95%	66.70%	65.06%	–
Ours (WRN-28-10)				89.48%	64.08%	62.76%	62.80%
Augustin et al. (2020) (ResNet-50)				91.08%	–	–	72.91%
Ours (WRN-70-16)	CIFAR-10	$\ell_2$	$\epsilon = 128/255$	94.74%	82.19%	80.45%	<b>80.53%</b>
Hendrycks et al. (2019) (ResNet-18)				59.23%	–	–	28.42%
Ours (WRN-70-16)	CIFAR-100	$\ell_\infty$	$\epsilon = 8/255$	69.15%	38.97%	37.70%	<b>36.88%</b>

## References

- Maksym Andriushchenko and Nicolas Flammarion. Understanding and Improving Fast Adversarial Training. *Adv. Neural Inform. Process. Syst.*, 2020.
- Maksym Andriushchenko, Francesco Croce, Nicolas Flammarion, and Matthias Hein. Square Attack: a query-efficient black-box adversarial attack via random search. *Eur. Conf. Comput. Vis.*, 2020.
- Anish Athalye and Ilya Sutskever. Synthesizing robust adversarial examples. *Int. Conf. Mach. Learn.*, 2018.
- Anish Athalye, Nicholas Carlini, and David Wagner. Obfuscated gradients give a false sense of security: Circumventing defenses to adversarial examples. *Int. Conf. Mach. Learn.*, 2018.
- Maximilian Augustin, Alexander Meinke, and Matthias Hein. Adversarial Robustness on In-and Out-Distribution Improves Explainability. *Eur. Conf. Comput. Vis.*, 2020.
- Yogesh Balaji, Tom Goldstein, and Judy Hoffman. Instance adaptive adversarial training: Improved accuracy tradeoffs in neural nets. 2019. URL <https://openreview.net/pdf?id=SyeOVTEFPH>.
- Mariusz Bojarski, Davide Del Testa, Daniel Dworakowski, Bernhard Firner, Beat Flepp, Praseon Goyal, Lawrence D. Jackel, Mathew Monfort, Urs Muller, Jiakai Zhang, Xin Zhang, Jake Zhao, and Karol Zieba. End to end learning for self-driving cars. *NIPS Deep Learning Symposium*, 2016.
- James Bradbury, Roy Frostig, Peter Hawkins, Matthew James Johnson, Chris Leary, Dougal Maclaurin, and Skye Wanderman-Milne. JAX: composable transformations of Python+NumPy programs, 2018. URL <http://github.com/google/jax>.
- Jacob Buckman, Aurko Roy, Colin Raffel, and Ian Goodfellow. Thermometer Encoding: One Hot Way To Resist Adversarial Examples. In *Int. Conf. Learn. Represent.*, 2018.
- Nicholas Carlini. Is AmI (Attacks Meet Interpretability) Robust to Adversarial Examples? *arXiv preprint arXiv:1902.02322*, 2019.
- Nicholas Carlini and David Wagner. Defensive Distillation is Not Robust to Adversarial Examples. *arXiv preprint arXiv:1607.04311*, 2016.
- Nicholas Carlini and David Wagner. Adversarial examples are not easily detected: Bypassing ten detection methods. In *Proceedings of the 10th ACM Workshop on Artificial Intelligence and Security*, pp. 3–14. ACM, 2017a.
- Nicholas Carlini and David Wagner. Towards evaluating the robustness of neural networks. In *2017 IEEE Symposium on Security and Privacy*, 2017b.
- Nicholas Carlini, Anish Athalye, Nicolas Papernot, Wieland Brendel, Jonas Rauber, Dimitris Tsipras, Ian Goodfellow, and Aleksander Madry. On Evaluating Adversarial Robustness. *arXiv preprint arXiv:1902.06705*, 2019.
- Yair Carmon, Aditi Raghunathan, Ludwig Schmidt, John C Duchi, and Percy S Liang. Unlabeled data improves adversarial robustness. In *Adv. Neural Inform. Process. Syst.*, 2019.
- Tianlong Chen, Zhenyu Zhang, Sijia Liu, Shiyu Chang, and Zhangyang Wang. Robust overfitting may be mitigated by properly learned smoothening. In *Int. Conf. Learn. Represent.*, 2021. URL <https://openreview.net/pdf?id=qZzy5urZw9>.

- Ting Chen, Simon Kornblith, Mohammad Norouzi, and Geoffrey Hinton. A simple framework for contrastive learning of visual representations. *Int. Conf. Mach. Learn.*, 2020.
- Djork-Arné Clevert, Thomas Unterthiner, and Sepp Hochreiter. Fast and accurate deep network learning by exponential linear units (elus). *Int. Conf. Learn. Represent.*, 2016.
- Jeremy M Cohen, Elan Rosenfeld, and J Zico Kolter. Certified Adversarial Robustness via Randomized Smoothing. *Int. Conf. Mach. Learn.*, 2019.
- Paul Covington, Jay Adams, and Emre Sargin. Deep neural networks for YouTube recommendations. In *Proceedings of the 10th ACM Conference on Recommender Systems*, 2016.
- Francesco Croce and Matthias Hein. Reliable evaluation of adversarial robustness with an ensemble of diverse parameter-free attacks. *arXiv preprint arXiv:2003.01690*, 2020.
- Ekin D Cubuk, Barret Zoph, Dandelion Mane, Vijay Vasudevan, and Quoc V Le. Autoaugment: Learning augmentation policies from data. *IEEE Conf. Comput. Vis. Pattern Recog.*, 2019.
- Ekin D. Cubuk, Barret Zoph, Jonathon Shlens, and Quoc V. Le. Randaugment: Practical automated data augmentation with a reduced search space. *IEEE Conf. Comput. Vis. Pattern Recog.*, 2020.
- Jeffrey De Fauw, Joseph R Ledsam, Bernardino Romera-Paredes, Stanislav Nikolov, Nenad Tomasev, Sam Blackwell, Harry Askham, Xavier Glorot, Brendan O’Donoghue, Daniel Visentin, George van den Driessche, Balaji Lakshminarayanan, Clemens Meyer, Faith Mackinder, Simon Bouton, Kareem Ayoub, Reena Chopra, Dominic King, Alan Karthikesalingam, Cían O Hughes, Rosalind Raine, Julian Hughes, Dawn A Sim, Catherine Egan, Adnan Tufail, Hugh Montgomery, Demis Hassabis, Geraint Rees, Trevor Back, Peng T Khaw, Mustafa Suleyman, Julien Cornebise, Pearse A Keane, and Olaf Ronneberger. Clinically applicable deep learning for diagnosis and referral in retinal disease. In *Nature Medicine*, 2018.
- Terrance DeVries and Graham W Taylor. Improved regularization of convolutional neural networks with cutout. *arXiv preprint arXiv:1708.04552*, 2017.
- Yinpeng Dong, Fangzhou Liao, Tianyu Pang, Hang Su, Jun Zhu, Xiaolin Hu, and Jianguo Li. Boosting Adversarial Attacks with Momentum. *IEEE Conf. Comput. Vis. Pattern Recog.*, 2018.
- Stefan Elfving, Eiji Uchibe, and Kenji Doya. Sigmoid-weighted linear units for neural network function approximation in reinforcement learning. *Neural Networks*, 2018.
- Logan Engstrom, Andrew Ilyas, and Anish Athalye. Evaluating and Understanding the Robustness of Adversarial Logit Pairing. *arXiv preprint arXiv:1807.10272*, 2018.
- Logan Engstrom, Andrew Ilyas, Hadi Salman, Shibani Santurkar, and Dimitris Tsipras. Robustness (python library), 2019. URL <https://github.com/MadryLab/robustness>.
- Reuben Feinman, Ryan R. Curtin, Saurabh Shintre, and Andrew B. Gardner. Detecting Adversarial Samples from Artifacts. *arXiv preprint arXiv:1703.00410*, 2017.
- Ian Goodfellow, Yoshua Bengio, and Aaron Courville. *Deep Learning*. MIT Press, 2016. URL <http://www.deeplearningbook.org>.
- Ian J Goodfellow, Jonathon Shlens, and Christian Szegedy. Explaining and harnessing adversarial examples. *Int. Conf. Learn. Represent.*, 2015.



- Sven Gowal, Krishnamurthy Dvijotham, Robert Stanforth, Rudy Bunel, Chongli Qin, Jonathan Uesato, Relja Arandjelovic, Timothy Mann, and Pushmeet Kohli. Scalable verified training for provably robust image classification. *Int. Conf. Comput. Vis.*, 2019a.
- Sven Gowal, Jonathan Uesato, Chongli Qin, Po-Sen Huang, Timothy Mann, and Pushmeet Kohli. An Alternative Surrogate Loss for PGD-based Adversarial Testing. *arXiv preprint arXiv:1910.09338*, 2019b.
- Priya Goyal, Piotr Dollár, Ross Girshick, Pieter Noordhuis, Lukasz Wesolowski, Aapo Kyrola, Andrew Tulloch, Yangqing Jia, and Kaiming He. Accurate, large minibatch sgd: Training imagenet in 1 hour. *arXiv preprint arXiv:1706.02677*, 2017.
- Chuan Guo, Mayank Rana, Moustapha Cisse, and Laurens van der Maaten. Countering Adversarial Images using Input Transformations. *Int. Conf. Learn. Represent.*, 2018.
- Kaiming He, Xiangyu Zhang, Shaoqing Ren, and Jian Sun. Deep residual learning for image recognition. *IEEE Conf. Comput. Vis. Pattern Recog.*, 2016.
- Dan Hendrycks and Kevin Gimpel. Gaussian error linear units (gelus). *arXiv preprint arXiv:1606.08415*, 2016.
- Dan Hendrycks, Kimin Lee, and Mantas Mazeika. Using Pre-Training Can Improve Model Robustness and Uncertainty. *Int. Conf. Mach. Learn.*, 2019.
- Dan Hendrycks, Norman Mu, Ekin D. Cubuk, Barret Zoph, Justin Gilmer, and Balaji Lakshminarayanan. Augmix: A simple data processing method to improve robustness and uncertainty. *Int. Conf. Learn. Represent.*, 2020.
- Tom Hennigan, Trevor Cai, Tamara Norman, and Igor Babuschkin. Haiku: Sonnet for JAX, 2020. URL <http://github.com/deepmind/dm-haiku>.
- Geoffrey Hinton, Li Deng, Dong Yu, George E Dahl, Abdel-rahman Mohamed, Navdeep Jaitly, Andrew Senior, Vincent Vanhoucke, Patrick Nguyen, Tara N Sainath, and others. Deep neural networks for acoustic modeling in speech recognition: The shared views of four research groups. *IEEE Signal processing magazine*, 29(6):82–97, 2012.
- Lang Huang, Chao Zhang, and Hongyang Zhang. Self-Adaptive Training: beyond Empirical Risk Minimization. *arXiv preprint arXiv:2002.10319*, 2020.
- Pavel Izmailov, Dmitrii Podoprikin, Timur Garipov, Dmitry Vetrov, and Andrew Gordon Wilson. Averaging Weights Leads to Wider Optima and Better Generalization. *Uncertainty in Artificial Intelligence*, 2018.
- Rafal Jozefowicz, Wojciech Zaremba, and Ilya Sutskever. An empirical exploration of recurrent network architectures. In *Int. Conf. Mach. Learn.*, 2015.
- Harini Kannan, Alexey Kurakin, and Ian Goodfellow. Adversarial Logit Pairing. *arXiv preprint arXiv:1803.06373*, 2018.
- Alex Krizhevsky, Ilya Sutskever, and Geoffrey E Hinton. Imagenet classification with deep convolutional neural networks. In *Adv. Neural Inform. Process. Syst.*, 2012.
- Alexey Kurakin, Ian Goodfellow, and Samy Bengio. Adversarial examples in the physical world. *ICLR workshop*, 2016.
- Yanpei Liu, Xinyun Chen, Chang Liu, and Dawn Song. Delving into transferable adversarial examples and black-box attacks. *Int. Conf. Learn. Represent.*, 2017.

- Ilya Loshchilov and Frank Hutter. SGDR: stochastic gradient descent with warm restarts. In *Int. Conf. Learn. Represent.*, 2017.
- Jiajun Lu, Hussein Sibai, Evan Fabry, and David Forsyth. NO Need to Worry about Adversarial Examples in Object Detection in Autonomous Vehicles. *IEEE Conf. Comput. Vis. Pattern Recog.*, 2017.
- Andrew L Maas, Awni Y Hannun, and Andrew Y Ng. Rectifier nonlinearities improve neural network acoustic models. In *Int. Conf. Mach. Learn.*, 2013.
- Aleksander Madry, Aleksandar Makelov, Ludwig Schmidt, Dimitris Tsipras, and Adrian Vladu. Towards deep learning models resistant to adversarial attacks. *Int. Conf. Learn. Represent.*, 2018.
- Jan Hendrik Metzen, Tim Genewein, Volker Fischer, and Bastian Bischoff. On Detecting Adversarial Perturbations. *Int. Conf. Learn. Represent.*, 2017.
- Matthew Mirman, Timon Gehr, and Martin Vechev. Differentiable Abstract Interpretation for Provably Robust Neural Networks. In *Int. Conf. Mach. Learn.*, 2018.
- Seyed-Mohsen Moosavi-Dezfooli, Alhussein Fawzi, Jonathan Uesato, and Pascal Frossard. Robustness via curvature regularization, and vice versa. *IEEE Conf. Comput. Vis. Pattern Recog.*, 2019.
- Marius Mosbach, Maksym Andriushchenko, Thomas Trost, Matthias Hein, and Dietrich Klakow. Logit Pairing Methods Can Fool Gradient-Based Attacks. *arXiv preprint arXiv:1810.12042*, 2018.
- Vinod Nair and Geoffrey E. Hinton. Rectified linear units improve restricted boltzmann machines. In *Int. Conf. Mach. Learn.*, 2010.
- Amir Najafi, Shin-ichi Maeda, Masanori Koyama, and Takeru Miyato. Robustness to adversarial perturbations in learning from incomplete data. *Adv. Neural Inform. Process. Syst.*, 2019.
- Yurii Nesterov. A method of solving a convex programming problem with convergence rate  $o(1/k^2)$ . In *Sov. Math. Dokl*, 1983.
- Avital Oliver, Augustus Odena, Colin Raffel, Ekin D. Cubuk, and Ian J. Goodfellow. Realistic evaluation of deep semi-supervised learning algorithms. *Adv. Neural Inform. Process. Syst.*, 2018.
- Tianyu Pang, Kun Xu, Chao Du, Ning Chen, and Jun Zhu. Improving adversarial robustness via promoting ensemble diversity. *Int. Conf. Mach. Learn.*, 2019.
- Tianyu Pang, Xiao Yang, Yinpeng Dong, Hang Su, and Jun Zhu. Bag of tricks for adversarial training. *arXiv preprint arXiv:2010.00467*, 2020a.
- Tianyu Pang, Xiao Yang, Yinpeng Dong, Kun Xu, Hang Su, and Jun Zhu. Boosting Adversarial Training with Hypersphere Embedding. *Adv. Neural Inform. Process. Syst.*, 2020b.
- Nicolas Papernot, Patrick McDaniel, Xi Wu, Somesh Jha, and Ananthram Swami. Distillation as a defense to adversarial perturbations against deep neural networks. *IEEE Symposium on Security and Privacy*, 2016.
- Boris T Polyak. Some methods of speeding up the convergence of iteration methods. *USSR Computational Mathematics and Mathematical Physics*, 1964.
- Chongli Qin, James Martens, Sven Gowal, Dilip Krishnan, Krishnamurthy Dvijotham, Alhussein Fawzi, Soham De, Robert Stanforth, and Pushmeet Kohli. Adversarial Robustness through Local Linearization. *Adv. Neural Inform. Process. Syst.*, 2019.

- Colin Raffel, Noam Shazeer, Adam Roberts, Katherine Lee, Sharan Narang, Michael Matena, Yanqi Zhou, Wei Li, and Peter J. Liu. Exploring the limits of transfer learning with a unified text-to-text transformer. *J. Mach. Learn. Res.*, 2020.
- Prajit Ramachandran, Barret Zoph, and Quoc V. Le. Searching for activation functions. *arXiv preprint arXiv:1710.05941*, 2017.
- Leslie Rice, Eric Wong, and J. Zico Kolter. Overfitting in adversarially robust deep learning. *Int. Conf. Mach. Learn.*, 2020.
- Hadi Salman, Greg Yang, Jerry Li, Pengchuan Zhang, Huan Zhang, Ilya Razenshteyn, and Sebastien Bubeck. Provably Robust Deep Learning via Adversarially Trained Smoothed Classifiers. *Adv. Neural Inform. Process. Syst.*, 2019.
- Ludwig Schmidt, Shibani Santurkar, Dimitris Tsipras, Kunal Talwar, and Aleksander Madry. Adversarially Robust Generalization Requires More Data. In *Adv. Neural Inform. Process. Syst.* 2018.
- Vikash Sehwal, Shiqi Wang, Prateek Mittal, and Suman Jana. Hydra: Pruning adversarially robust neural networks. *Adv. Neural Inform. Process. Syst.*, 2020.
- Thilo Strauss, Markus Hanselmann, Andrej Junginger, and Holger Ulmer. Ensemble methods as a defense to adversarial perturbations against deep neural networks. *arXiv preprint arXiv:1709.03423*, 2017.
- Christian Szegedy, Wojciech Zaremba, Ilya Sutskever, Joan Bruna, Dumitru Erhan, Ian Goodfellow, and Rob Fergus. Intriguing properties of neural networks. *Int. Conf. Learn. Represent.*, 2014.
- Mingxing Tan and Quoc V. Le. Efficientnet: Rethinking model scaling for convolutional neural networks. *Int. Conf. Mach. Learn.*, 2019.
- Guanhong Tao, Shiqing Ma, Yingqi Liu, and Xiangyu Zhang. Attacks Meet Interpretability: Attribute-steered Detection of Adversarial Samples. *Adv. Neural Inform. Process. Syst.*, 2018.
- Antonio Torralba, Rob Fergus, and William T. Freeman. 80 million tiny images: a large dataset for non-parametric object and scene recognition. *IEEE Trans. Pattern Anal. Mach. Intell.*, 2008.
- Florian Tramèr, Alexey Kurakin, Nicolas Papernot, Ian Goodfellow, Dan Boneh, and Patrick McDaniel. Ensemble Adversarial Training: Attacks and Defenses. *arXiv preprint arXiv:1705.07204*, 2017. URL <https://arxiv.org/pdf/1705.07204>.
- Jonathan Uesato, Brendan O’Donoghue, Aaron van den Oord, and Pushmeet Kohli. Adversarial Risk and the Dangers of Evaluating Against Weak Attacks. *Int. Conf. Mach. Learn.*, 2018.
- Jonathan Uesato, Jean-Baptiste Alayrac, Po-Sen Huang, Robert Stanforth, Alhussein Fawzi, and Pushmeet Kohli. Are labels required for improving adversarial robustness? *Adv. Neural Inform. Process. Syst.*, 2019.
- Yisen Wang, Difan Zou, Jinfeng Yi, James Bailey, Xingjun Ma, and Quanquan Gu. Improving adversarial robustness requires revisiting misclassified examples. In *Int. Conf. Learn. Represent.*, 2020.
- Eric Wong, Frank Schmidt, Jan Hendrik Metzen, and J Zico Kolter. Scaling provable adversarial defenses. *Adv. Neural Inform. Process. Syst.*, 2018.
- Eric Wong, Leslie Rice, and J. Zico Kolter. Fast is better than free: Revisiting adversarial training. *Int. Conf. Learn. Represent.*, 2020.

- Dongxian Wu, Shu-tao Xia, and Yisen Wang. Adversarial weight perturbation helps robust generalization. *Adv. Neural Inform. Process. Syst.*, 2020.
- Kai Y Xiao, Vincent Tjeng, Nur Muhammad Shafiullah, and Aleksander Madry. Training for Faster Adversarial Robustness Verification via Inducing ReLU Stability. *Int. Conf. Learn. Represent.*, 2019.
- Cihang Xie and Alan Yuille. Intriguing properties of adversarial training. *arXiv:1906.03787*, 2019. URL <http://arxiv.org/pdf/1906.03787>.
- Cihang Xie and Alan Yuille. Intriguing properties of adversarial training at scale. *Int. Conf. Learn. Represent.*, 2020.
- Cihang Xie, Yuxin Wu, Laurens van der Maaten, Alan Yuille, and Kaiming He. Feature denoising for improving adversarial robustness. *IEEE Conf. Comput. Vis. Pattern Recog.*, 2019.
- Cihang Xie, Mingxing Tan, Boqing Gong, Alan Yuille, and Quoc V. Le. Smooth adversarial training. *arXiv preprint arXiv:2006.14536*, 2020a.
- Cihang Xie, Mingxing Tan, Boqing Gong, Alan Yuille, and Quoc V. Le. Smooth Adversarial Training. *arXiv preprint arXiv:2006.14536*, 2020b.
- Sergey Zagoruyko and Nikos Komodakis. Wide residual networks. *Brit. Mach. Vis. Conf.*, 2016.
- Runtian Zhai, Tianle Cai, Di He, Chen Dan, Kun He, John Hopcroft, and Liwei Wang. Adversarially Robust Generalization Just Requires More Unlabeled Data. *arXiv preprint arXiv:1906.00555*, 2019.
- Haichao Zhang and Jianyu Wang. Defense Against Adversarial Attacks Using Feature Scattering-based Adversarial Training. *Adv. Neural Inform. Process. Syst.*, 2019.
- Hongyang Zhang, Yaodong Yu, Jiantao Jiao, Eric P. Xing, Laurent El Ghaoui, and Michael I. Jordan. Theoretically Principled Trade-off between Robustness and Accuracy. *Int. Conf. Mach. Learn.*, 2019.
- Hongyi Zhang, Moustapha Cisse, Yann N Dauphin, and David Lopez-Paz. mixup: Beyond empirical risk minimization. *Int. Conf. Learn. Represent.*, 2018.
- Huan Zhang, Hongge Chen, Chaowei Xiao, Sven Gowal, Robert Stanforth, Bo Li, Duane Boning, and Cho-Jui Hsieh. Towards Stable and Efficient Training of Verifiably Robust Neural Networks. *Int. Conf. Learn. Represent.*, 2020.
- Daniel Zoran, Mike Chrzanowski, Po-Sen Huang, Sven Gowal, Alex Mott, and Pushmeet Kohli. Towards Robust Image Classification Using Sequential Attention Models. *IEEE Conf. Comput. Vis. Pattern Recog.*, 2019.

## A. Additional experiments

In order to keep the main text concise, we relegated additional experiments to this section. Similarly to [section 4](#), each section is self-contained to allow the reader to jump to any section of interest. The outline is as follows:

A.1	Outer minimization	21
A.1.1	Learning rate schedule	21
A.1.2	Number of optimization steps	22
A.1.3	$\ell_2$ regularization	23
A.2	Inner maximization	23
A.2.1	Number of optimization steps	23
A.2.2	Inner maximization perturbation radius (continued)	23
A.3	Additional unlabeled data	24
A.3.1	Ratio of labeled-to-unlabeled data per batch (continued)	24
A.3.2	Label smoothing	25
A.4	Other tricks	25
A.4.1	Batch size	25
A.4.2	Data augmentation	26
A.4.3	Label smoothing	27

### A.1. Outer minimization

#### A.1.1. Learning rate schedule

In this section, we test different learning rate schedules. In particular, we compare the *multistep* schedule introduced in [subsection 3.1](#), where the initial learning rate of 0.1 is decayed by 10 $\times$  half-way and three-quarters-of-the-way through training, with the *cosine* and *exponential* schedules. For the *cosine* schedule, we set the initial learning rate to 0.1 and decay it to 0 by the end of training. For the *exponential* schedule, we set the initial learning rate to 0.1 and decay it every 5 epochs such that by the end of training the final learning rate is 0.001. Learning rates are all scaled according to the batch size (i.e., effective learning = max(learning rate  $\times$  batch size/256, learning rate)).

**Results.** [Table 6](#) shows that, as they are currently implemented, the *multistep* schedule is superior to the *cosine* and *exponential* schedules. While, we did our best to tune all schedules, we do not exclude the possibility that better schedules exist. In particular, the optimal schedule may depend on the model architecture and method used to find adversarial examples (e.g., AT or TRADES). Smoother schedules

Table 6 | Clean (without perturbations) and robust (under adversarial attack) accuracy obtained by different learning rate schedules trained on CIFAR-10 (with and without additional unlabeled data) against  $\ell_\infty$  norm-bounded perturbations of size  $\epsilon = 8/255$ .

SETUP	CIFAR-10		with 80M-TI	
	CLEAN	ROBUST	CLEAN	ROBUST
LEARNING RATE SCHEDULE				
Multistep decay	84.85 $\pm$ 1.20%	50.80 $\pm$ 0.23%	90.93 $\pm$ 0.25%	58.41 $\pm$ 0.25%
Cosine	83.90%	47.49%	91.28%	57.87%
Exponential	83.39%	47.73%	91.08%	56.56%

Table 7 | Clean (without perturbations) and robust (under adversarial attack) accuracy obtained for different number of training epochs trained on CIFAR-10 (with and without additional unlabeled data) against  $\ell_\infty$  norm-bounded perturbations of size  $\epsilon = 8/255$ .

SETUP	CIFAR-10		with 80M-Ti	
	CLEAN	ROBUST	CLEAN	ROBUST
NUMBER OF TRAINING EPOCHS				
50	78.83%	47.25%	–	–
100	84.30%	49.89%	85.62%	53.20%
200	84.85±1.20%	50.80±0.23%	89.74%	57.37%
400	83.11%	50.16%	90.93±0.25%	58.41±0.25%
800	–	–	91.09%	56.98%

(like *cosine* or *exponential*) are also less sensitive to the early stopping criterion and may result in less noisy results. When using additional unlabeled data, model weight averaging (subsubsection 4.5.1) and a WRN-70-16, we found that the *cosine* schedule performed slightly better than the *multistep* schedule (+0.24%).

**Key takeaways.** The *multistep* schedule developed over the years, which has been tuned to Wide-ResNets and adversarial training, works well for settings with and without additional unlabeled data.

### A.1.2. Number of optimization steps

Training for longer is not always beneficial, especially when it comes to adversarial training. The robust overfitting phenomenon studied by Rice et al. (2020) attests to the difficulty of finding the right number of steps to optimize for. In this experiment, we use the *multistep* learning rate schedule and change the number of training epochs. We expect to find an optimal schedule that balances overfitting with robustness.

**Results.** In Table 7, we vary the number of training epochs between {50, 100, 200, 400} for the setting without additional data and between {100, 200, 400, 800} for the setting with additional data. For both settings, training for longer is not beneficial. Without additional data, using 400 epochs instead of 200 leads to degradation of the robust accuracy by -0.64%. With additional data, using 800 epochs instead of 400 leads to degradation of -1.43%. Figure 6 shows the robust accuracy as training progresses for the setting without additional data. We observe that letting the model train for longer leads to robust overfitting.

**Key takeaways.** Robust training (with adversarial training) does not benefit from longer training times. The phenomenon of robust overfitting (Rice

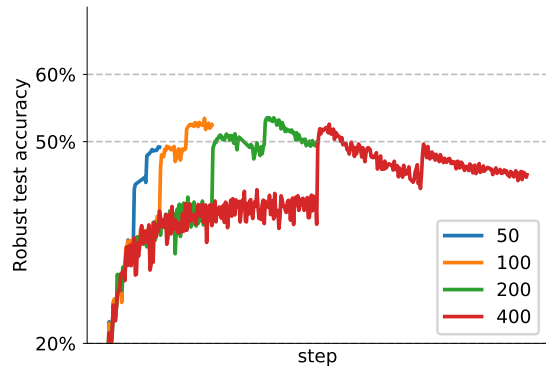


Figure 6 | Accuracy under  $\ell_\infty$  attacks of size  $\epsilon = 8/255$  on CIFAR-10 as we vary the number of training epochs (without additional unlabeled data) against PGD<sup>40</sup>.

et al., 2020) can lead to reduced performance. As such, it is important to balance the number of training epochs with other hyperparameters (such as  $\ell_2$  regularization).

### A.1.3. $\ell_2$ regularization

For completeness, we also explore explicit regularization using  $\ell_2$  regularization on the model weights. In this experiment, we vary the weight decay parameter between zero and  $5 \cdot 10^{-3}$ .

**Results.** Figure 7 (and Table 18 in Appendix C) demonstrates that there exists an ideal weight decay value. In particular, the best decay of  $5 \cdot 10^{-4}$  works well across both data settings (with and without additional data). This value is also the value used frequently in the literature when training adversarially robust Wide-ResNets (Carmon et al., 2019; Rice et al., 2020; Uesato et al., 2019; Wong et al., 2020). Without any  $\ell_2$  regularization, the robust accuracy drops by -5.06% (in the setting without additional data).

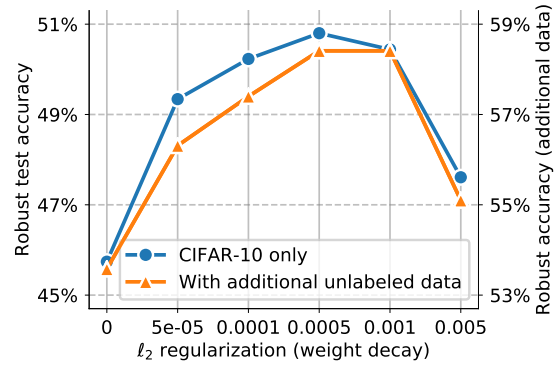


Figure 7 | Accuracy under  $\ell_\infty$  attacks of size  $\epsilon = 8/255$  on CIFAR-10 as we vary weight decay.

**Key takeaways.**  $\ell_2$  regularization is an important element of adversarial training. Further fine-grained tuning could improve robustness (albeit to a limited extent).

## A.2. Inner maximization

### A.2.1. Number of optimization steps

It is important that the attack used during training be strong enough. Weak attacks tend to provide a false sense of security by allowing the trained network to use obfuscation as a defense mechanism (Qin et al., 2019). In this experiment, we study the effect of the attack strength on robustness. Although recent work demonstrated that it is possible to train robust model with single-step attacks (Wong et al., 2020), it is generally accepted that the number of steps used for the inner optimization correlates with the strength of that optimization procedure (i.e., its ability to find a minima close to the global minima). Note, however, that more inner steps leads to increased training time.

**Results.** In Table 8, we vary the number of attack steps  $K$  between 1 and 16. We adapt the step-size by setting  $\alpha$  to  $\max(1.25\epsilon/K, 0.007)$ . We observe that stronger attacks yield more robust models (with diminishing returns). For example, increasing  $K$  from 4 to 8, 8 to 10 and 10 to 16 improves robust accuracy by +2.59%, +0.75% and +0.51% respectively (in the setting without additional data).

**Key takeaways.** Strong inner optimizations improve robustness (at the cost of increased training time).

### A.2.2. Inner maximization perturbation radius (continued)

This section continues the evaluation made in subsection 4.2.2. In particular, we evaluate the effect of using a larger perturbation radius within TRADES (Zhang et al., 2019) (subsection 4.2.2 explored this effect within classical adversarial training).

Table 8 | Clean (without perturbations) and robust (under adversarial attack) accuracy obtained when increasing the number of steps used for the inner optimization, trained on CIFAR-10 (with and without additional unlabeled data) against  $\ell_\infty$  norm-bounded perturbations of size  $\epsilon = 8/255$ .

SETUP	CIFAR-10		with 80M-TI	
	CLEAN	ROBUST	CLEAN	ROBUST
NUMBER OF INNER OPTIMIZATION STEPS				
$K = 1, \alpha = 10/255$	70.31%	33.48%	76.64%	41.79%
$K = 2, \alpha = 5/255$	87.84%	47.75%	92.34%	53.93%
$K = 4, \alpha = 2.5/255$	87.98%	47.91%	91.80%	55.49%
$K = 8, \alpha = 0.007$	86.32%	50.05%	90.99%	57.93%
$K = 10, \alpha = 0.007$	84.85±1.20%	50.80±0.23%	90.93±0.25%	58.41±0.25%
$K = 16, \alpha = 0.007$	85.90%	51.31%	90.73%	58.87%

Table 9 | Clean (without perturbations) and robust (under adversarial attack) accuracy obtained on CIFAR-10 (with and without additional unlabeled data) against  $\ell_\infty$  norm-bounded perturbations of size  $\epsilon = 8/255$  when using different perturbation radii for the inner maximization trained.

SETUP	CIFAR-10		with 80M-TI	
	CLEAN	ROBUST	CLEAN	ROBUST
PERTURBATION RADIUS USED FOR TRAINING WITH TRADES				
TRADES $\epsilon = 8/255$ (Zhang et al., 2019)	82.74%	51.91%	88.36%	59.45%
TRADES $\epsilon = 8.8/255$	82.93%	52.80%	86.86%	59.21%
TRADES $\epsilon = 9.6/255$	81.85%	52.50%	85.79%	58.64%

**Results.** Table 9 shows the effect of increasing the perturbation radius  $\epsilon$  by a factor  $1.1\times$  and  $1.2\times$  the original value of  $8/255$  (during training, not during evaluation). We notice that to the contrary of adversarial training, which benefits from increases perturbation radii, TRADES’ performance is inconsistent (possibly because TRADES is already actively managing the trade-off with clean accuracy).

**Key takeaways.** When using TRADES, tuning the perturbation radius is not always beneficial.

### A.3. Additional unlabeled data

#### A.3.1. Ratio of labeled-to-unlabeled data per batch (continued)

This section continues the evaluation made in subsection 4.3.2. We evaluate the effect of varying the labeled-to-unlabeled data ratio on our largest unlabeled dataset consisting of 1M images.

**Results.** Figure 8 shows the robust accuracy as we vary that ratio. Similarly to Figure 2 (which used the dataset from Carmon et al., 2019), we observe that giving slightly more importance to unlabeled data helps. We find an identical opti-

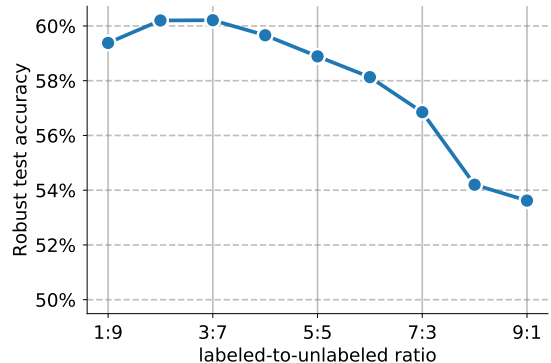


Figure 8 | Accuracy under  $\ell_\infty$  attacks of size  $\epsilon = 8/255$  on CIFAR-10 as we vary the ratio of labeled-to-unlabeled data using our unlabeled datasets of 1M images.



Table 10 | Clean (without perturbations) and robust (under adversarial attack) accuracy obtained for different label smoothing factors (on unlabeled data only) trained on CIFAR-10 (with and without additional unlabeled data) against  $\ell_\infty$  norm-bounded perturbations of size  $\epsilon = 8/255$ .

SETUP	CIFAR-10		with 80M-Ti	
	CLEAN	ROBUST	CLEAN	ROBUST
LABEL SMOOTHING FOR THE ADDITIONAL UNLABELED DATA				
$\gamma = 0$	84.85±1.20%	50.80±0.23%	90.93±0.25%	58.41±0.25%
$\gamma = 0.01$	–	–	91.02%	57.97%
$\gamma = 0.02$	–	–	91.35%	57.98%
$\gamma = 0.05$	–	–	91.08%	57.65%
$\gamma = 0.1$	–	–	91.20%	57.72%
$\gamma = 0.2$	–	–	90.83%	58.10%

mal ratio of labeled-to-unlabeled data of 3:7, which provides a boost of +1.32% over the 1:1 ratio. When we use the dataset from Carmon et al. (2019), the optimal ratio provides a boost of +0.95% only. This could indicate that larger gains in robustness are possible when using larger unlabeled datasets.

**Key takeaways.** Larger unlabeled datasets can provide larger improvements in robustness.

### A.3.2. Label smoothing

As hinted in subsection 4.3.2, we experiment with label smoothing (for the additional unlabeled data). Label smoothing should counteract the effect of the noisy labels resulting from the classifier used in the *pseudo-labeling* process. Label smoothing modifies one-hot labels  $y$  by creating smoother targets  $\hat{y} = (1 - \gamma)y + \gamma 1$ . More specifically, we minimize the following loss

$$\mathcal{L}_\theta^{\text{AT-smooth}} = l_{\text{xent}}(f(x + \hat{\delta}; \theta), \hat{y}), \quad \text{where } \hat{\delta} \approx \arg \max_{\delta \in \mathcal{S}} l_{\text{xent}}(f(x + \delta; \theta), y). \quad (8)$$

**Results.** In Table 10, we apply label smoothing to the examples originating from the additional unlabeled dataset (from Carmon et al., 2019). We vary  $\gamma$  for these examples only (i.e., the labeled data from CIFAR-10 continues to use hard labels with  $\gamma = 0$ ). We observe that label smoothing is detrimental and that the resulting robust accuracy is inconsistent, without a clear correlation with  $\gamma$ .

**Key takeaways.** Applying label smoothing to the additional unlabeled data is detrimental to robustness.

## A.4. Other tricks

### A.4.1. Batch size

Using larger batch size not only influences resource utilization but also affects the optimization process. Larger batches provide less noisy gradients (e.g., when using Stochastic Gradient Descent) and more precise batch statistics. In classical adversarial training, it is common to let the batch statistics “float” as the inner optimization process is run.<sup>10</sup> As such, batch size also influences the quality of the adversarial examples generated during training. In this experiment, we vary the batch size and compensate for the

<sup>10</sup>Xie & Yuille (2019) experimented with alternative batch normalization strategies.

loss of gradient noise by scaling the outer learning rate using the linear scaling rule introduced by Goyal et al. (2017) (i.e., effective learning =  $\max(\text{learning rate} \times \text{batch size}/256, \text{learning rate})$ ).

**Results.** Table 11 shows the robust accuracy resulting from using different batch sizes. We observe that our default batch size of 128 is sub-optimal for the setting without additional unlabeled data: a batch size of 512 improves robust accuracy by +0.88%. For the setting with additional unlabeled data, the largest batch size (i.e., 1024) remains the best, as it improves on smaller batch sizes by at least +0.66%.

**Key takeaways.** Training batch size has an effect on robustness.

#### A.4.2. Data augmentation

Data augmentation can reduce generalization error. For image classification tasks, random flips, rotations and crops are commonly used (He et al., 2016). As is common for CIFAR-10, in our baseline settings, we apply random translations by up to 4 pixels and random horizontal flips. More sophisticated techniques such as *Cutout* (DeVries & Taylor, 2017) (which produces random occlusions) and *mixup* (Zhang et al., 2018) (which linearly interpolates between two images) demonstrate compelling results on standard classification tasks. However, both techniques are not very effective when used in conjunction with adversarial training (Rice et al., 2020). In this experiment, we evaluate *AutoAugment* (Cubuk et al., 2019), *RandAugment* (Cubuk et al., 2020) and the *AugMix* augmentation (Hendrycks et al., 2020) (with their default settings). We also evaluate the color augmentation scheme proposed by Chen et al. (2020) (as part of the *SimCLR* pipeline) by varying the *color jittering* strength. Irrespective of the strength, this color augmentation scheme always includes a random color drop (i.e., conversion to gray-scale) with a probability of 20%.

**Results.** Table 12 summarizes the results. We observe that *AutoAugment*, *RandAugment* and *AugMix*, which have mainly been tuned for IMAGENET, reduce robust accuracy. These techniques would require further fine-tuning to be competitive with the simplest augmentation scheme (i.e., random translation by 4 pixels). Furthermore, we observe that increasing the strength of *color jittering* correlates negatively with robustness, as robust accuracy drops by -1.98% and -1.50% in the settings without and with additional data, respectively. Finally, we note that randomly dropping color does improve robustness in both settings (i.e., +0.69% and +0.29% with respect to the baselines).

**Key takeaways.** Data augmentation schemes that perform well for standard classification tasks do not necessarily improve robust generalization.

Table 11 | Clean (without perturbations) and robust (under adversarial attack) accuracy obtained for batch sizes trained on CIFAR-10 (with and without additional unlabeled data) against  $\ell_\infty$  norm-bounded perturbations of size  $\epsilon = 8/255$ .

SETUP	CIFAR-10		with 80M-TI	
	CLEAN	ROBUST	CLEAN	ROBUST
BATCH SIZE				
128	84.85±1.20%	50.80±0.23%	90.13%	56.71%
256	83.39%	50.74%	90.71%	57.57%
512	83.31%	51.68%	90.96%	57.75%
1024	83.54%	50.60%	90.93±0.25%	58.41±0.25%

Table 12 | Clean (without perturbations) and robust (under adversarial attack) accuracy obtained for different data augmentation schemes trained on CIFAR-10 (with and without additional unlabeled data) against  $\ell_\infty$  norm-bounded perturbations of size  $\epsilon = 8/255$ .

SETUP	CIFAR-10		with 80M-TI	
	CLEAN	ROBUST	CLEAN	ROBUST
DATA AUGMENTATION				
default = translate(4) + flip(0.5)	84.85±1.20%	50.80±0.23%	90.93±0.25%	58.41±0.25%
<i>AutoAugment</i> (Cubuk et al., 2019)	86.24%	50.37%	90.21%	56.57%
<i>RandAugment</i> (Cubuk et al., 2020)	85.01%	47.37%	88.93%	52.48%
<i>AugMix</i> (Hendrycks et al., 2020)	82.05%	50.12%	89.67%	56.62%
default + color-jitter(0) (Chen et al., 2020)	84.29%	51.49%	90.53%	58.70%
default + color-jitter(0.1) (Chen et al., 2020)	84.19%	50.87%	91.05%	58.27%
default + color-jitter(0.2) (Chen et al., 2020)	83.80%	51.10%	90.97%	58.43%
default + color-jitter(0.3) (Chen et al., 2020)	82.87%	50.89%	91.05%	57.98%
default + color-jitter(0.4) (Chen et al., 2020)	83.42%	50.01%	91.24%	57.04%
default + color-jitter(0.5) (Chen et al., 2020)	83.43%	49.51%	90.79%	57.20%

#### A.4.3. Label smoothing

In this section, we complement the label smoothing experiment done in [subsubsection A.3.2](#). To the contrary of [subsubsection A.3.2](#), which explored label smoothing for unlabeled data only, this section explores label smoothing for the labeled data.

**Results.** [Table 13](#) shows the results. We do not observe any clear correlation between label smoothing and robust accuracy. In particular, setting the label smoothing factor  $\gamma$  to 0.02 and 0.2 seems helpful (in both data settings), while setting it to 0.05 or 0.1 seems detrimental in at least one of the two data settings.

**Key takeaways.** Applying label smoothing to the labeled data has minor effects on robustness.

Table 13 | Clean (without perturbations) and robust (under adversarial attack) accuracy obtained for different label smoothing factors (on labeled data only) trained on CIFAR-10 (with and without additional unlabeled data) against  $\ell_\infty$  norm-bounded perturbations of size  $\epsilon = 8/255$ .

SETUP	CIFAR-10		with 80M-TI	
	CLEAN	ROBUST	CLEAN	ROBUST
LABEL SMOOTHING FOR THE LABELED DATA				
$\gamma = 0$	84.85±1.20%	50.80±0.23%	90.93±0.25%	58.41±0.25%
$\gamma = 0.01$	84.39%	50.65%	90.50%	58.86%
$\gamma = 0.02$	82.88%	51.13%	91.11%	58.46%
$\gamma = 0.05$	83.85%	50.91%	90.82%	58.34%
$\gamma = 0.1$	84.09%	50.26%	91.28%	58.66%
$\gamma = 0.2$	83.49%	51.25%	90.70%	58.89%

## B. Comparison with concurrent works

Independently of our work, [Pang et al. \(2020a\)](#)<sup>11</sup> also investigate the limits of current approaches to adversarial training. We also highlight concurrent works by [Chen et al. \(2021\)](#)<sup>12</sup> and [Wu et al. \(2020\)](#)[Wu et al. \(2020\)](#)<sup>13</sup>. We briefly summarize both these works here for clarity and completeness.

[Pang et al. \(2020a\)](#). This work is the closest in essence to ours. [Pang et al. \(2020a\)](#) make a thorough literature review and observe that different papers on adversarial robustness differ in their hyperparameters (despite using similar techniques). While they analyze some properties that we also analyze in this manuscript (such as training batch size, label smoothing, weight decay, activation functions), they also complement our analyses with experiments on early stopping and perturbation radius warm-up, optimizers, model architectures beyond Wide-ResNets and batch normalization. The combination of their findings applied to a WRN-34-20 reaches 54.39% robust accuracy without additional unlabeled data (in comparison, our WRN-34-20 reaches a robust accuracy of 56.86%). Their study hints at further improvements by more finely tuning the weight decay.

[Wu et al. \(2020\)](#). In their manuscript, [Wu et al. \(2020\)](#) explore *adversarial weight perturbation* as way to improve robust generalization. Their technique interleaves model weight perturbations with example perturbations (within a single training step). They observe that the resulting loss landscapes become flatter and, as a result, robustness improves. Using this approach, [Wu et al. \(2020\)](#) improve robust accuracy by significant margins reaching 56.17% without additional data. By combining our findings with their technique, we expect that further improvements are possible (although we posit that model weight averaging may already have a similar effect).

[Chen et al. \(2021\)](#). Simultaneously to us, [Chen et al. \(2021\)](#) discovered that model weight averaging can significantly improve robustness on a wide range of models and datasets. They argue (similarly to [Wu et al., 2020](#)) that WA leads to a flatter adversarial loss landscape, and thus a smaller robust generalization gap. In addition to matching our experimental results on WA, they provide a deeper, noteworthy analysis.

---

<sup>11</sup>Accepted to the 2021 Conference on Learning Representations and available on ArXiv on October 1st, 2020.

<sup>12</sup>Accepted to the 2021 Conference on Learning Representations and available on OpenReview on September 28th, 2020.

<sup>13</sup>Accepted at the 2020 Conference on Neural Information Processing Systems, but only available in its final form (with their latest results) from ArXiv on October 13th, 2020.

### C. Additional detailed results

Table 14 | Clean (without perturbations) and robust (under adversarial attack) accuracy obtained by different network sizes trained on CIFAR-10 (with and without additional unlabeled data) against  $\ell_\infty$  norm-bounded perturbations of size  $\epsilon = 8/255$ .

SETUP	CIFAR-10		with 80M-TI	
	CLEAN	ROBUST	CLEAN	ROBUST
<b>NETWORK WIDTH AND DEPTH</b>				
WRN-28-10	84.85±1.20%	50.80±0.23%	90.93±0.25%	58.41±0.25%
WRN-28-15	86.91%	51.79%	91.71%	59.81%
WRN-28-20	86.87%	51.78%	91.63%	59.90%
WRN-34-10	86.42%	51.18%	91.45%	58.52%
WRN-34-15	86.40%	51.12%	91.84%	59.61%
WRN-34-20	87.32%	52.91%	92.14%	60.90%
WRN-40-10	86.27%	51.89%	91.47%	59.47%
WRN-40-15	86.94%	52.18%	91.66%	60.44%
WRN-40-20	86.62%	53.19%	91.98%	60.97%
WRN-46-10	85.98%	52.02%	91.71%	59.40%
WRN-46-15	86.73%	52.74%	91.78%	60.56%
WRN-46-20	87.22%	53.24%	92.08%	61.14%

Table 15 | Clean (without perturbations) and robust (under adversarial attack) accuracy obtained by weight averaging decay values trained on CIFAR-10 (with and without additional unlabeled data) against  $\ell_\infty$  norm-bounded perturbations of size  $\epsilon = 8/255$ .

SETUP	CIFAR-10		with 80M-TI	
	CLEAN	ROBUST	CLEAN	ROBUST
<b>MODEL WEIGHT AVERAGING</b>				
No weight averaging	84.85±1.20%	50.80±0.23%	90.93±0.25%	58.41±0.25%
Decay parameter $\tau = 0.95$	85.48%	50.46%	91.07%	58.12%
$\tau = 0.9625$	85.80%	50.53%	91.28%	58.23%
$\tau = 0.975$	86.34%	50.65%	91.03%	58.37%
$\tau = 0.9875$	83.47%	51.45%	91.09%	58.33%
$\tau = 0.99$	83.41%	51.37%	91.51%	58.69%
$\tau = 0.9925$	86.08%	51.44%	91.23%	58.74%
$\tau = 0.995$	84.41%	52.10%	90.28%	59.14%
$\tau = 0.9975$	84.91%	52.31%	91.28%	58.19%
$\tau = 0.999$	84.62%	52.21%	91.66%	57.16%

Table 16 | Clean (without perturbations) and robust (under adversarial attack) accuracy obtained by different activations trained on CIFAR-10 (with and without additional unlabeled data) against  $\ell_\infty$  norm-bounded perturbations of size  $\epsilon = 8/255$ .

SETUP	CIFAR-10		with 80M-TI	
	CLEAN	ROBUST	CLEAN	ROBUST
ACTIVATION				
ReLU (Nair & Hinton, 2010)	84.85±1.20%	50.80±0.23%	90.93±0.25%	58.41±0.25%
Swish/SiLU (Hendrycks & Gimpel, 2016)	85.60%	51.40%	91.03%	59.54%
Leaky ReLU (Maas et al., 2013)	85.21%	51.00%	90.77%	58.55%
ELU (Clevert et al., 2016)	81.87%	49.20%	89.13%	56.48%
Softplus	83.59%	50.61%	89.87%	57.83%
GELU (Hendrycks & Gimpel, 2016)	85.67%	50.66%	91.09%	59.37%

Table 17 | Clean (without perturbations) and robust (under adversarial attack) accuracy obtained using ratios of labeled-to-unlabeled data on CIFAR-10 and 80M-TI against  $\ell_\infty$  norm-bounded perturbations of size  $\epsilon = 8/255$ .

SETUP	CIFAR-10		with 80M-TI	
	CLEAN	ROBUST	CLEAN	ROBUST
WEIGHTING OF UNLABELED DATA (ratio of labeled-to-unlabeled data per batch)				
10:0 (more labeled data)	84.85±1.20%	50.80±0.23%	–	–
9:1	–	–	88.60%	51.79%
8:2	–	–	86.74%	53.27%
7:3	–	–	90.37%	56.58%
6:4	–	–	90.85%	57.19%
5:5	–	–	90.93±0.25%	58.41±0.25%
4:6	–	–	91.06%	59.04%
3:7	–	–	90.99%	59.36%
2:8	–	–	90.69%	59.13%
1:9 (more unlabeled data)	–	–	90.57%	58.06%

Table 18 | Clean (without perturbations) and robust (under adversarial attack) accuracy obtained for different weight decays trained on CIFAR-10 (with and without additional unlabeled data) against  $\ell_\infty$  norm-bounded perturbations of size  $\epsilon = 8/255$ .

SETUP	CIFAR-10		with 80M-TI	
	CLEAN	ROBUST	CLEAN	ROBUST
NUMBER OF TRAINING EPOCHS				
0	78.69%	45.74%	88.82%	53.58%
$5 \cdot 10^{-5}$	84.95%	49.34%	90.98%	56.31%
$1 \cdot 10^{-4}$	85.04%	50.72%	89.99%	57.40%
$5 \cdot 10^{-4}$	84.85±1.20%	50.80±0.23%	90.93±0.25%	58.41±0.25%
$1 \cdot 10^{-3}$	85.16%	50.44%	90.61%	58.41%
$5 \cdot 10^{-3}$	79.47%	47.61%	86.60%	55.10%

## D. Loss landscape analysis

In this section, we analyze the adversarial loss landscapes of two of our best models trained without and with additional data against  $\ell_\infty$  norm-bounded perturbations of size  $8/255$  on CIFAR-10. As a comparison, we also show the loss landscapes of the model trained by Carmon et al. (2019). This analysis complements the black-box Square attack Andriushchenko et al. (2020) used by AUTOATTACK. To generate a loss landscape, we vary the network input along the linear space defined by the worse perturbation found by PGD<sup>40</sup> ( $u$  direction) and a random Rademacher direction ( $v$  direction). The  $u$  and  $v$  axes represent the magnitude of the perturbation added in each of these directions respectively and the  $z$  axis is the adversarial margin loss (Carlini & Wagner, 2017b):  $z_y - \max_{i \neq y} z_i$  (i.e., a misclassification occurs when this value falls below zero).

Figure 9, Figure 10 and Figure 11 shows the loss landscapes around the first 5 images of the CIFAR-10 test set for our largest model trained with additional unlabeled data, our largest model trained without additional unlabeled data and Carmon et al.’s model trained with additional unlabeled data, respectively. Most landscapes are smooth and do not exhibit patterns of gradient obfuscation. Interestingly, the landscapes corresponding to the fifth image (of a dog) are quite similar across all models, with the larger models’ landscapes being less smooth (with a cliff). Overall, it is difficult to interpret these figures further and we rely on the fact that AUTOATTACK and MULTITARGETED are accurate. We note that the black-box Square attack Andriushchenko et al. (2020) does not find any misclassified attack that was not already found by AUTOPGD and MULTITARGETED.

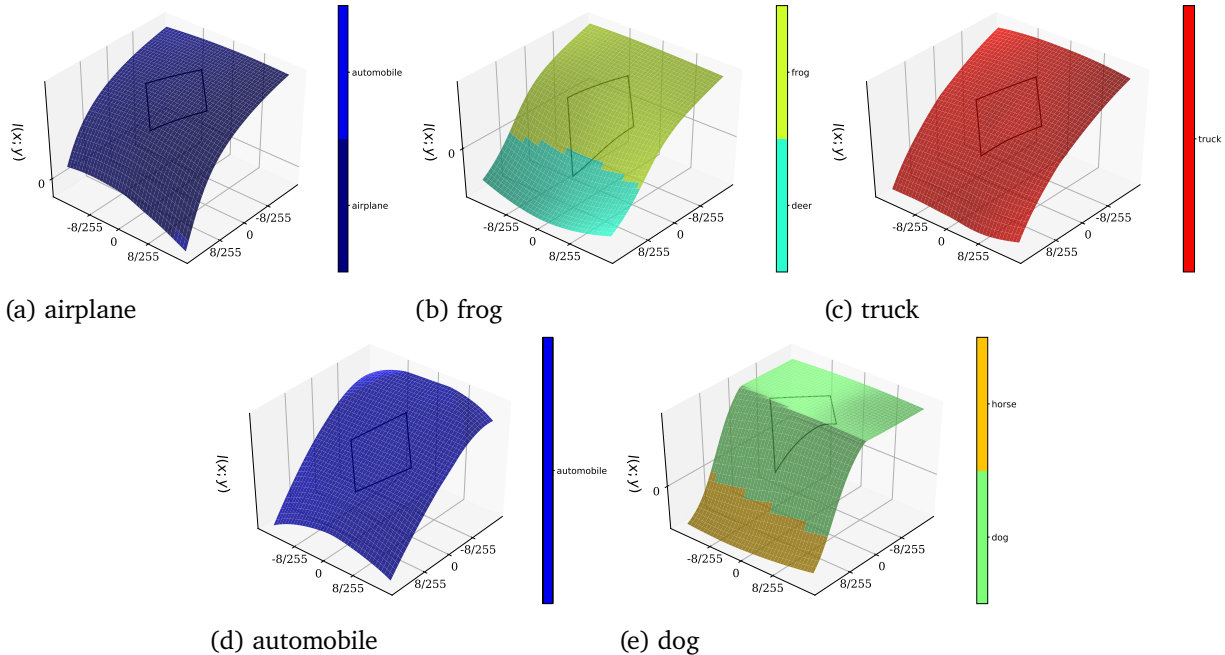


Figure 9 | Loss landscapes around different CIFAR-10 test images. It is generated by varying the input to the model, starting from the original input image toward either the worst attack found using PGD<sup>40</sup> ( $u$  direction) or a random Rademacher direction ( $v$  direction). The loss used for these plots is the margin loss  $z_y - \max_{i \neq y} z_i$  (i.e., a misclassification occurs when this value falls below zero). The model used is our WRN-70-16 trained with additional unlabeled data against  $\ell_\infty$  norm-bounded perturbations of size  $8/255$  on CIFAR-10. The diamond-shape represents the projected  $\ell_\infty$  ball of size  $\epsilon = 8/255$  around the nominal image.

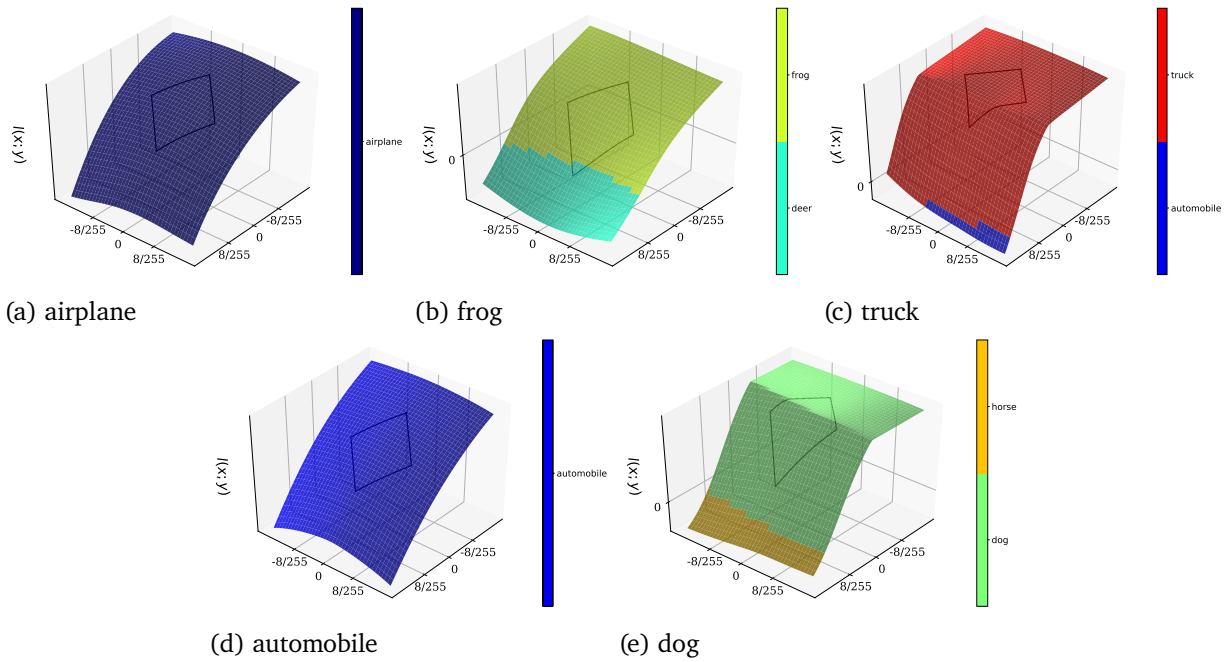


Figure 10 | Loss landscapes around different CIFAR-10 test images. It is generated by varying the input to the model, starting from the original input image toward either the worst attack found using PGD<sup>40</sup> ( $u$  direction) or a random Rademacher direction ( $v$  direction). The loss used for these plots is the margin loss  $z_y - \max_{i \neq y} z_i$  (i.e., a misclassification occurs when this value falls below zero). The model used is our WRN-70-16 trained without additional unlabeled data against  $\ell_\infty$  norm-bounded perturbations of size  $8/255$  on CIFAR-10. The diamond-shape represents the projected  $\ell_\infty$  ball of size  $\epsilon = 8/255$  around the nominal image.



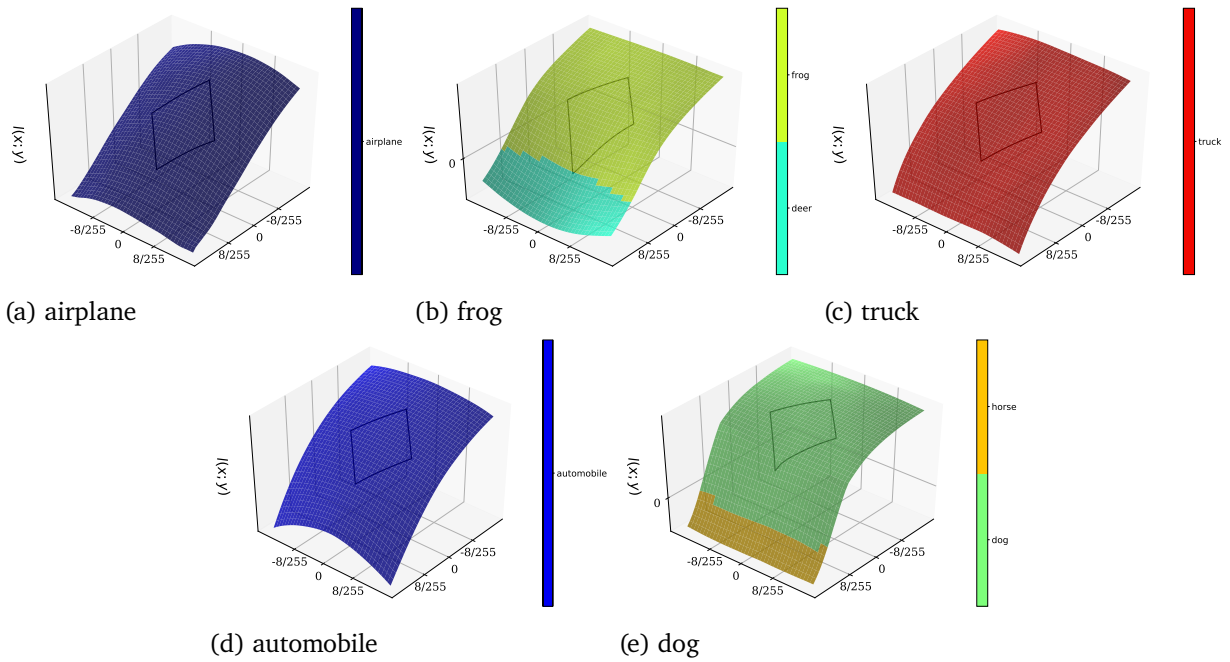


Figure 11 | Loss landscapes around different CIFAR-10 test images. It is generated by varying the input to the model, starting from the original input image toward either the worst attack found using PGD<sup>40</sup> ( $u$  direction) or a random Rademacher direction ( $v$  direction). The loss used for these plots is the margin loss  $z_y - \max_{i \neq y} z_i$  (i.e., a misclassification occurs when this value falls below zero). The model used is Carmon et al.’s WRN-28-10 model trained with additional unlabeled data against  $\ell_\infty$  norm-bounded perturbations of size  $8/255$  on CIFAR-10. The diamond-shape represents the projected  $\ell_\infty$  ball of size  $\epsilon = 8/255$  around the nominal image.